# TARGETING POWER GENERATION FROM WASTE HEAT STREAMS

A Thesis

by

OMAR AHMAD AL-ANI

Submitted to the Office of Graduate and Professional Studies of
Texas A&M University
in partial fulfillment of the requirements for the degree of

MASTER OF SCIENCE

| | |
|---|---|
| Chair of Committee, | Patrick Linke |
| Committee Members, | Marcelo Castier |
| | Reza Sadr |
| Head of Department, | M. Nazmul Karim |

May 2017

Major Subject: Chemical Engineering

ABSTRACT

The paper proposes two procedures to target thermodynamic power generation limits from a set of heat source streams. The first procedure takes the form of an algebraic targeting approach commonly applied in process heat integration. This procedure is based on fundamental thermodynamics laws and the Carnot cycle. The procedure allows the designer to quickly determine the maximum amount of power that can theoretically be generated from the available heat in thermodynamic cycles. The second procedure uses the Rankine cycle to determine the amount of power that can be generated using a real power generating cycle. The paper describes both procedures and their applicability in the context of common data availability for heat source streams in the form of Composite Curves or Total Site Profiles (hot composites) commonly developed in heat integration. The application of both procedures is illustrated with examples.

DEDICATION

To my parents

# ACKNOWLEDGEMENTS

I would like to thank my committee chair, Dr. Patrick Linke, and my committee members, Dr. Marcelo Castier and Dr. Reza Sadr, for their guidance and support throughout the course of this research.

CONTRIBUTORS AND FUNDING SOURCES

This work was supervised by a thesis committee consisting of Dr. Patrick Linke [advisor] and Dr. Marcelo Castier of the Department of Chemical Engineering and Dr. Reza Sadr of Mechanical Engineering.

All work for the thesis was completed independently by the student.

There are no outside funding contributions to acknowledge related to the research and compilation of this document.

NOMENCLATURE

| | |
|---|---|
| $CP_j$ | Heat capacity of interval *j* |
| $dW$ | Infinitesimal power generated |
| $dQ$ | Infinitesimal heat source |
| $dT$ | Infinitesimal temperature difference |
| $DT$ | Temperature step size |
| $h_1$ | Enthalpy of working fluid after the preheater in a Rankine cycle |
| $h_2$ | Enthalpy of working fluid before the turbine in a Rankine cycle |
| $h_3$ | Enthalpy of working fluid after the turbine in a Rankine cycle |
| $h_4$ | Enthalpy of working fluid after the condenser in a Rankine cycle |
| $h_5$ | Enthalpy of working fluid before the preheater in a Rankine cycle |
| $H_{v,j}$ | Latent heat of interval *j* |
| $m_i$ | Mass flow rate of working fluid at evaporation temperature *i* |
| $P_{out}$ | Pressure after turbine |
| $P_{sat}, i$ | Saturation pressure for evaporation temperature *i* |
| $Q_i$ | Heat used for evaporation temperature *i* |
| $Q_j$ | Heat available in interval *j* |
| $Q_{E,R}$ | Evaporator heat used by Rankine cycle |
| $Q_{P,R}$ | Preheater heat used by Rankine cycle |
| $Q_{T,R}$ | Total heat used by Rankine cycle |
| $\Delta T$ | Minimum acceptable temperature difference |

| | |
|---|---|
| $T_0$ | Minimum temperature of a Rankine cycle |
| $T_{eff}$ | Evaporation temperature with highest Rankine cycle efficiency |
| $T_H$ | Temperature of high temperature reservoir |
| $T_i$ | Inlet temperature of interval *i* |
| $T_{i+1}$ | Exit temperature of interval *i* |
| $T_L$ | Temperature of low temperature reservoir |
| $T_s$ | Initial temperature of a hot stream |
| $T_f$ | Final temperature of a hot stream |
| $T_P$ | Temperature at preheater |
| $W_j$ | Power generated in interval *j* |
| $W_j^{max}$ | Maximum power generated from interval *j* |
| $W_{max}$ | Maximum power generated from Rankine targeting method |
| $W_R$ | Power generated by Rankine cycle |
| $\eta_c$ | Carnot cycle efficiency |
| $\eta_{c,j}$ | Carnot cycle efficiency of interval *j* |
| $\eta_i$ | Rankine cycle efficiency for evaporation temperature *i* |
| $\eta_j^{max}$ | Maximum Carnot efficiency for an interval |
| $\eta_R$ | Rankine cycle efficiency |
| $\eta_{sys}^{max}$ | Maximum Carnot efficiency for a waste heat stream system |

TABLE OF CONTENTS


| | Page |
|---|---|
| ABSTRACT | ii |
| DEDICATION | iii |
| ACKNOWLEDGEMENTS | iv |
| CONTRIBUTORS AND FUNDING SOURCES | v |
| NOMENCLATURE | vi |
| TABLE OF CONTENTS | viii |
| LIST OF FIGURES | x |
| LIST OF TABLES | xii |
| CHAPTER I INTRODUCTION | 1 |
| CHAPTER II LITERATURE REVIEW | 5 |
| CHAPTER III BACKGROUND | 10 |
| 3.1 Introduction | 10 |
| 3.2 Carnot Cycle | 10 |
| 3.3 Rankine Cycle | 12 |
| 3.4 Composite Curves | 16 |
| 3.5 Targeting | 17 |
| CHAPTER IV CARNOT CYCLE TARGETING | 18 |
| 4.1 Introduction | 18 |
| 4.2 Problem Statement and Basic Relationships | 18 |
| 4.3 Algebraic Targeting Approach | 24 |
| 4.4 Illustrative Examples | 26 |
| 4.5 Comparison between Targeting Individual and Composite Streams | 32 |
| CHAPTER V RANKINE CYCLE TARGETING | 34 |
| 5.1 Introduction | 34 |
| 5.2 Single Stream Matching Procedure | 34 |

5.3 Individual Stream Targeting Illustrative Case Study .................................... 45
5.4 Multiple Stream Matching Procedure ........................................................... 48
5.5 Multiple Stream Illustrative Case Study ...................................................... 50
5.6 Comparison between Individual Stream Matching and Multiple Stream Matching……………………………………………………………………… 52
5.7 Effect of Step Size on $W_{max}$…… ................................................................. 56

CHAPTER VI SUMMARY AND CONCLUSIONS............................................ 58

REFERENCES.......................................................................................... 60

APPENDIX A .......................................................................................... 64

APPENDIX B .......................................................................................... 66

LIST OF FIGURES


Page

Figure 1 Waste Heat on Composite Curve ............................................................ 2

Figure 2 Carnot Cycle Stages .................................................................................. 11

Figure 3 Rankine Cycle Stages ................................................................................. 13

Figure 4 Efficiency of Rankine Cycle with Respect to Evaporation Temperature . 15

Figure 5 Example of Composite Curve ................................................................... 16

Figure 6 Composite Curve for Multiple Hot Streams ............................................ 19

Figure 7 Lost Power Potential Due to Single Carnot Cycle ................................... 21

Figure 8 Power Generation Using Multiple Carnot Cycles .................................... 21

Figure 9 Example Problem Table ........................................................................... 25

Figure 10 Composite Curve for Carnot Cycle Illustrative Case Study .................. 29

Figure 11 Problem Table for Carnot Cycle Case Study 1 ....................................... 30

Figure 12 Problem Table for Carnot Cycle Case Study 2 ....................................... 31

Figure 13 Problem Table for Carnot Cycle Case Study 3 ....................................... 31

Figure 14 Infeasible and Feasible Heat Transfer ..................................................... 36

Figure 15 Using Two Rankine Cycles ..................................................................... 38

Figure 16 Using Three Rankine Cycles ................................................................... 40

Figure 17 Multiple Rankine Cycles Using Available Heat ...................................... 41

Figure 18 Flowchart for Matching Procedure .......................................................... 41

Figure 19 Preheating of All Rankine Cycles ............................................................ 43

Figure 20 Evaporating and Preheating of Rankine Cycles........................................ 44

Figure 21 Individual Stream Matching for Stream 1 ................................................ 46

Figure 22 Individual Stream Matching for Stream 2 ................................................ 47

Figure 23 Multiple Stream Matching Composite Curve ............................................ 49

Figure 24 Multiple Stream Matching of Case Study.................................................. 51

Figure 25 Stream 1 and Stream 2 “Composite” Curve ............................................. 53

Figure 26 Individual Stream Matching...................................................................... 54

Figure 27 Multiple Stream Matching ........................................................................ 55

LIST OF TABLES


Page

Table 1 Operating Conditions of Rankine Cycle .................................................. 13

Table 2 Streams Used for Carnot Cycle Illustrative Case Study ........................... 28

Table 3 Stream-by-Stream Analysis...................................................................... 32

Table 4 Rankine Targeting Case Study Streams ................................................... 45

Table 5 Individual Stream Targeting Results........................................................ 45

Table 6 Comparison between Carnot Cycle Targeting and Rankine Cycle Targeting ......................................................................................................... 47

Table 7 Multiple Stream Targeting Results .......................................................... 50

Table 8 Individual and Multiple Stream Cases ..................................................... 52

Table 9 Individual and Multiple Stream Cases Results ........................................ 53

Table 10 Results from Multiple Stream Matching.................................................. 55

Table 11 Effect of Step Size on Power Generated .................................................. 56

# CHAPTER I

# INTRODUCTION

Energy efficiency has become an increasingly important topic. Various methods have been suggested to reduce energy consumption. One method that has been suggested is to utilize low to medium temperature heat to generate power. Low to medium temperature heat can be extracted from multiple sources including geothermal, solar, and industrial waste heat [1]. The heat from these sources can be converted to power through the use of thermodynamic cycles. The most common method to convert low temperature heat into power is the Rankine Cycle.

In industrial processes, there are multiple streams that need to be cooled down or heated. A procedure known as heat integration is usually done to see if it is possible to use heat from the hot streams to heat up the cold streams. As a result, this would save utility costs by not needed to use cooling water or using steam. However, if there are too many hot streams and not enough cooling from the cold streams, the remaining heat is known as waste heat. The streams that make up this waste heat are known as waste heat streams. The waste heat can either be cooled down using cooling water. Alternatively, power can be generated from the waste heat streams. This waste heat is shown on a composite curve in Figure 1.

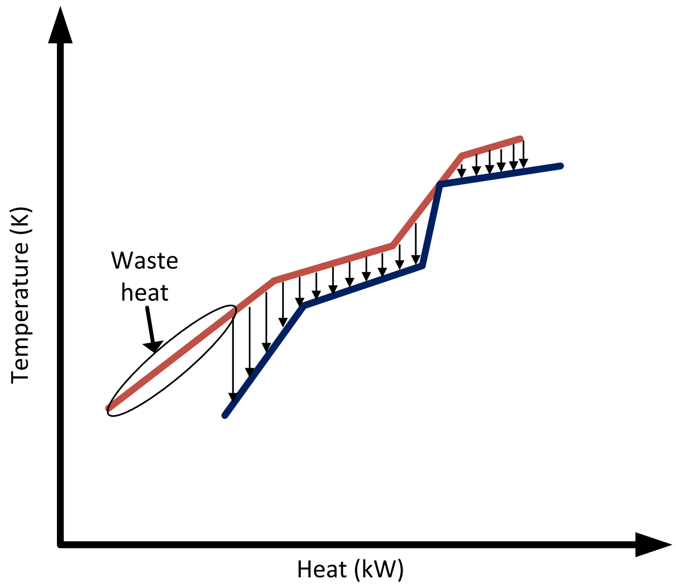


**Figure 1-Waste Heat on Composite Curve**

However, before converting heat into power, it is important to determine how much power can be generated from these heat sources. Otherwise, resources might be wasted on designing a system that would produce very little power. In order to determine how much power can be generated from heat sources, targeting needs to be done. Targeting is an important procedure in process optimization and has found many applications in heat integration, water integration, and mass integration [2]. Targeting in these applications is used to determine the minimum amount of utilities that is required. However, in power generation targeting, the goal is to determine the maximum amount of power that can be generated from a given heat source. By developing a methodology to determine a power generation target, it would be possible to know how much power can be generated before starting the design process. This would allow engineers and designers to determine if the project is feasible early on in the project planning process, thus saving money and time.

The methods that have been proposed in literature are not true targets since they do not determine the maximum amount of power that can be generated. This goal of this work is to provide a methodology which would determine "true" targets for power generation from heat sources. Two methods will be developed; one method based on the Carnot Cycle and the second method based on the Rankine Cycle.

Chapters 2 and 3 will introduce previous literature that has been done on this topic and include background information necessary to understand the methods and theories used in this work. Chapter 4 will focus on developing a targeting method to determine the maximum amount of power that can be generated from multiple heat sources. This will be done by using the definition of the Carnot efficiency. By using the heat content of the various heat sources, the maximum amount of power can be determined. This targeting method will allow designers to quickly determine the amount of power that can be theoretically generated. This would provide a baseline for designers to works towards. This targeting method uses many simplifying assumptions to make the procedure effortless. This targeting method will be used as a stepping stone to the second targeting method (that will be introduced in Chapter 5) which will use less simplifying assumptions and will be targeting towards using real power cycles. Chapter 5 will focus on developing a target method to determine the maximum amount of power that can be generated by real cycles. This targeting method uses the Rankine cycle as the power generation cycle. As this method uses the Rankine Cycle to generate power, two additional items are considered when determining the amount of power generated; the preheating of the working fluid and the thermophysical properties of the working fluid. By taking these two factors into account, a more realistic target will be determined. The target that will be determined by this method is the maximum amount of power that can be generated by a Rankine Cycle using a specific working fluid.

CHAPTER II

LITERATURE REVIEW

In light of the continuing shift towards sustainable industrial systems, low to medium grade heat to power conversion has become of increasing importance for low emissions electricity supply [1, 3-4]. Low to medium temperature heat source streams can be found in many systems including industrial processes, geothermal energy, biomass, and solar energy [5]. Particularly in the processes of the basic materials industries, many heat source streams exist that transfer excess heat into cold utilities such as cooling water or air at different temperatures. Rather than directly transferring heat into cold utilities, these streams could supply heat to thermodynamic cycles for zero emissions power generation. This work aims to quantify the maximum amount of power that could be generated from these hot streams (targeting) so as to help in quickly establishing the thermodynamic limits ahead of any detailed design work.

Targeting for minimum energy or mass requirements is a common activity in conceptual or process integration studies. Heat integration through Pinch Analysis has become a standard procedure to determine the maximum possible heat recovery within a process together with the minimum heating and cooling requirements [6]. Similar procedures have been proposed to analyze heat integration across multiple processes in an integrated site through Total Site Analysis [7-10]. In both Pinch and Total Site Analysis, multiple heat source streams are represented as composite profiles in T-H space from which targets can be easily determined from existing procedures either graphically [11] or from corresponding algebraic approaches [12-14]. There have been extensions to the heat integration approaches to assess heat and power options in process heat integration. Linnhoff and Dhole propose exergy composite curves to analyse low-temperature processes [15]. Most works consider site utility systems operating steam Rankine cycles. Castier presented a method to determine the minimum requirements for hot and cold utilities according to their temperatures [16]. Mavromatis developed the turbine hardware model in order to account for different variables including turbine size, load, and operating conditions [17]. Recently, Ghannadzadeh et al. proposed an approach to targeting co-generation in site-utility systems [18]. Goh et al. proposed a methodology to synthesize utility systems with the heat exchange network in order to minimize the total operating cost of a trigeneration system before going into the detailed design [19]. Kapil et al present a method to target cogeneration potential through a combination of bottom-up and top-down procedure to all of optimization of steam levels [20]. Alwi et al. presented a method to simultaneously target energy usage and utility placement in order to maximize energy recovery [21].

While the previously mentioned process integration approaches are very well developed for targeting of process energy recovery and co-generation in utility systems, i.e. within a processing facility or a site, simple targeting approaches do not exist to quickly quantify the thermodynamic limits for power generation from a set of hot streams. The situation that excess heat is ejected beyond the boundaries of an industrial facility or site, e.g. into air or cooling water, is often encountered in macroscopic energy systems analysis. This excess heat is typically ejected from multiple hot streams. Our proposed approach aims to quickly answer the following question: How much power could theoretically be generated from the set of hot streams?

A number of works aimed to determine the maximum amount of power that can be generated from a single heat source stream. In an early contribution, Curzon and Ahlborn analysed power generation potentials assuming a Carnot cycle [22]. Later, Ondrechen et al. [23] determined the power generation limit from a finite hot temperature reservoir and an isothermal cold temperature reservoir using an infinite number of parallel Carnot cycles. Ibrahim et al. [24], Baik et al. [25] and Park and Kim [26] employed a similar approach to determine numerically or analytically the maximum theoretical efficiency for a system with both a finite hot temperature reservoir and a finite cold temperature reservoir. These methods did not consider power generation from multiple heat sources.

There have been a few studies which use the Rankine cycle for targeting power generation. Most works concentrate on optimizing the use of the available heat to maximize power generation. However, this is not correct since a target has not been set. Without determining a target, it is not possible to determine how close you are to achieving the maximum amount of power that can be generated.

Many strategies have been used to try to optimize Organic Rankine Cycles. Some studies have changed the configurations of the cycle in order to generate more power. This includes using multiple turbines and reusing heat. Other studies have changed the operating parameters in the Rankine cycle including the turbine inlet pressure and the condition of the working fluid (transcritical or superheated). Stijepovic et al. suggested using an ORC that used multiple pressures to generate more power [27]. Anvari et al. suggested using an ORC to recover heat from a gas turbine in order to increase the thermodynamic efficiency [28]. Li et al. proposed using a parallel and series two-stage ORC to generate power and they found that the series two-stage ORC generated more power than the parallel two-stage ORC [29]. Sadeghi et al. evaluated the performance of an ORC that used different configurations including a simple ORC, a parallel two stage ORC, and a series two stage ORC while using zeotropic mixtures [30]. Li et al. also proposed using two stage evaporation in order to improve the performance of the ORC [29]. Yun et al. report on an ORC that uses dual expanders with different capacities to be able to recover and use heat over a wider variation of heat input [31].

In addition to changing the configuration of the ORC, studies have been done on optimization through working fluid selection. As the working fluid is an important component in the ORC, the working fluid used can be a major decider on the efficiency of the system. Sadeghi et al. performed optimization to select a working fluid from a variety of zeotropic mixtures [30]. Xu et al. investigated the use of different working fluids in both subcritical and supercritical conditions [32]. Papadopoulos et al. investigated the various properties that would make a working fluid suitable for use in an ORC. In addition, Papadopoulos et al. did another study for designing working fluids based on the economic efficiency [33]. Chagnon-Lessard et al. compared the performance of 36 working fluids in order to optimize subcritical and transcritical ORCs [34]. Frutiger et al. presented a methodology to select working fluids for ORC while taking into account property uncertainties [35]. Collings et al. suggest using a dynamic ORC where the working fluid's composition changes based on ambient conditions [36]. Brignoli and Brown present a method to evaluate working fluids that are "well-described" (considerable experimental data) and "not-so-well-described" (little or no experimental data) [37].

CHAPTER III

BACKGROUND

### 3.1 Introduction

In order to understand how the methodology in this work is developed, a few key concepts will be introduced in this section. Two thermodynamic cycles will be introduced; the Carnot and Rankine cycles. Understanding the difference between these two cycles is integral in knowing why two different targeting methods are needed. Composite curves and targeting are two important topics in process integration and will be used throughout this work. Composite curves will be used in this work to determine if heat can be transferred from the waste heat streams to the thermodynamic cycles. A basic of understanding of targeting will be given. This work will be targeting for power generation thus the usefulness and purpose of targeting will be explained.

### 3.2 Carnot Cycle

The objective of this work is to determine the maximum amount of power that can be generated from a set of waste heat streams. In order to convert heat into power, a thermodynamic cycle needs to be used. In this work, the Carnot cycle will be used. The Carnot cycle is an ideal thermodynamic cycle that has the highest efficiency of any thermodynamic cycle. The Carnot cycle operates between two isothermal reservoirs at temperatures $T_H$ and $T_L$.

It consists of four mechanically reversible stages:

- Isothermal expansion

- Adiabatic expansion
- Isothermal compression
- Adiabatic compression

These stages are shown in Figure 2.

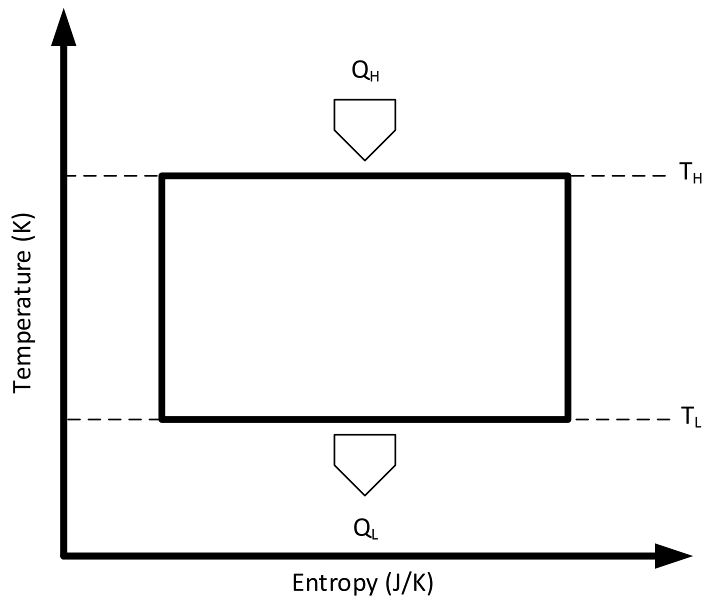


**Figure 2-Carnot Cycle Stages**

The efficiency of the Carnot cycle, known as the Carnot efficiency, can be calculated using Equation 1.

$$\eta = 1 - \frac{T_L}{T_H} \quad (1)$$

One of the features of the Carnot cycle is that it operates between two isothermal reservoirs. However, the heat sources that will be used in this work are not isothermal. This will be worked around in the next chapter.

In addition, a Carnot cycle is not a real cycle that can be made. The Carnot cycle assumes that all of the steps are reversible. However, this is not the case in real case situations. The stages are irreversible. As a result, the Carnot cycle is not a suitable thermodynamic cycle to use for real cases. The Rankine cycle is a more suitable cycle to use.

### 3.3 Rankine Cycle

Another thermodynamic cycle that will be used in this work is the Rankine cycle. The Rankine cycle is commonly used to generate power using water as its working fluid. However, it can also be used to generate power from low grade heat if a suitable working fluid is used. If a working fluid other than steam is used (usually an organic fluid), the cycle is called an Organic Rankine Cycle.

An ideal Rankine Cycle has five stages:

- Preheating
- Evaporating
- Adiabatic and Isentropic Expansion
- Condensing
- Adiabatic and Isentropic Compression

The operating conditions of the Rankine Cycle should be selected accordingly in order to increase the overall efficiency. In order to increase the efficiency of the Rankine Cycle, the main operating condition that is changed is the turbine inlet condition. Usually, the higher the temperature of the working fluid at the turbine inlet, the higher the efficiency of the cycle. The efficiency of the Rankine cycle is a function of the working fluid properties. As a result, the enthalpies of the fluid at different stages of the Rankine Cycle will be identified. Figure 3 shows the schematic of a Rankine cycle.

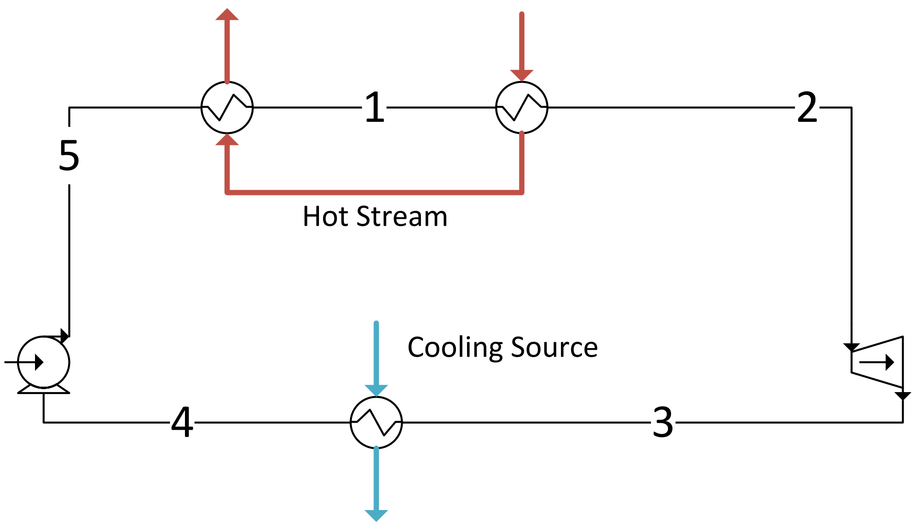


**Figure 3-Rankine Cycle Stages**

Each of the stages in the Rankine cycle has its own conditions. These are listed in Table 1.

**Table 1- Operating Conditions of Rankine Cycle**

| Stream | Enthalpy | Temperature (K) | Pressure (kPa) | Vapor Fraction |
|---|---|---|---|---|
| 1 | $h_1$ | $T_i$ | - | 0 |
| 2 | $h_2$ | $T_i$ | - | 1 |
| 3 | $h_3$ | - | $P_{out}$ | - |
| 4 | $h_4$ | $T_0+\Delta T$ | $P_{out}$ | 0 |
| 5 | $h_5$ | $T_0+\Delta T$ | $P_{sat}$ | - |

Where,

$T_i$ is the evaporation temperature [K]

$P_{sat}$ is the saturation pressure [Pa]

$T_0$ is the minimum temperature of the cycle [K]

$P_{out}$ is the pressure at the turbine outlet [Pa]

In this study, $T_0$ will be 298 K. The efficiency of the Rankine Cycle depends on the state of the working fluid before and after the turbine, and the amount of heat that is provided to the working fluid during preheating and evaporation. The efficiency of a Rankine Cycle can be calculated using Equation 2.

$$\eta_R = \frac{W}{Q_{T,R}} = \frac{W}{Q_p + Q_e} = \frac{h_2 - h_3}{(h_1 - h_5) - (h_2 - h_1)} \qquad (2)$$

Where,

$h_1$ is the enthalpy after the preheater (kJ/kg)

$h_2$ is the enthalpy before the turbine (kJ/kg)

$h_3$ is the enthalpy after the turbine (kJ/kg)

$h_5$ is the enthalpy before the preheater (kJ/kg)

Using Equation 2, the efficiency of the Rankine cycle for any evaporation temperature can be calculated. Each working fluid has a temperature, $T_{eff}$, in which the Rankine cycle has the maximum efficiency. A study was done using the CoolProp open source software in conjunction with MATLAB to determine the enthalpies of benzene for each stage in the Rankine cycle. The equation of state for benzene used in CoolProp is was developed by Thol et al [38].The efficiency of the Rankine cycle for various evaporation temperatures can be found. This can be seen from Figure 4 in which there is a temperature (557 K) in which the Rankine cycle has a maximum efficiency (33.33%) for benzene.

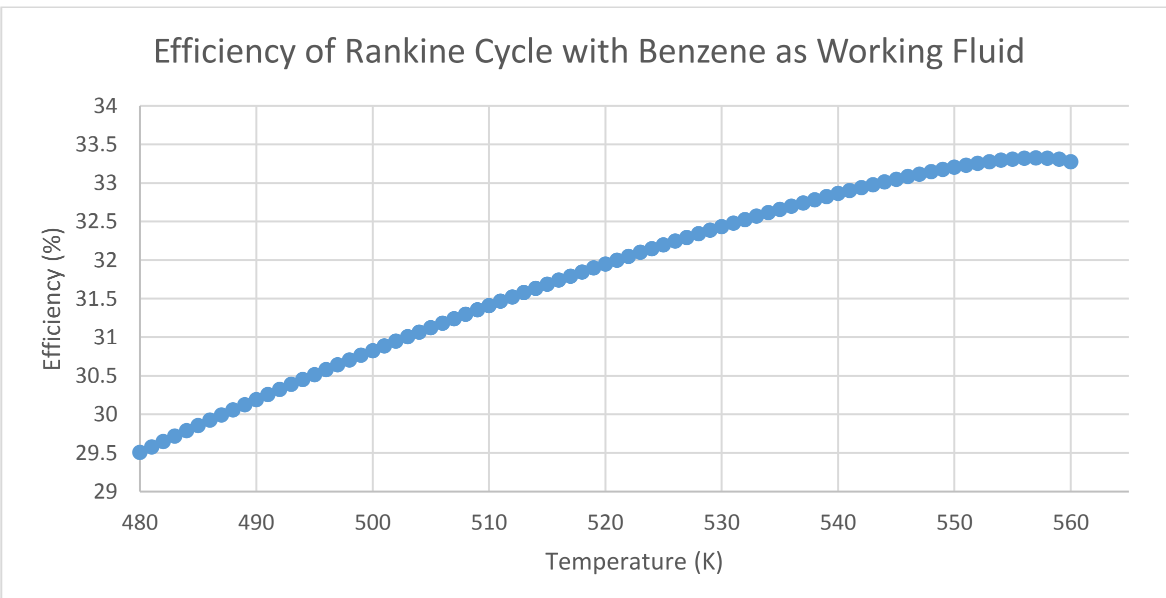


**Figure 4-Efficiency of Rankine Cycle with Respect to Evaporation Temperature**

### 3.4 Composite Curves

Composite curves are used in heat integration problems to determine where heat can be exchanged inside of a plant. There are two curves in a composite curve; a hot composite curve and a cold composite curve. The hot composite curve consists of those streams which need to be cooled down and the cold composite curve consists of those streams which need to be heated up. An example of a composite curve is shown in Figure 5. Composite curves will be used in this study to show how heat can be transferred from waste heat streams to Carnot and Rankine cycles.

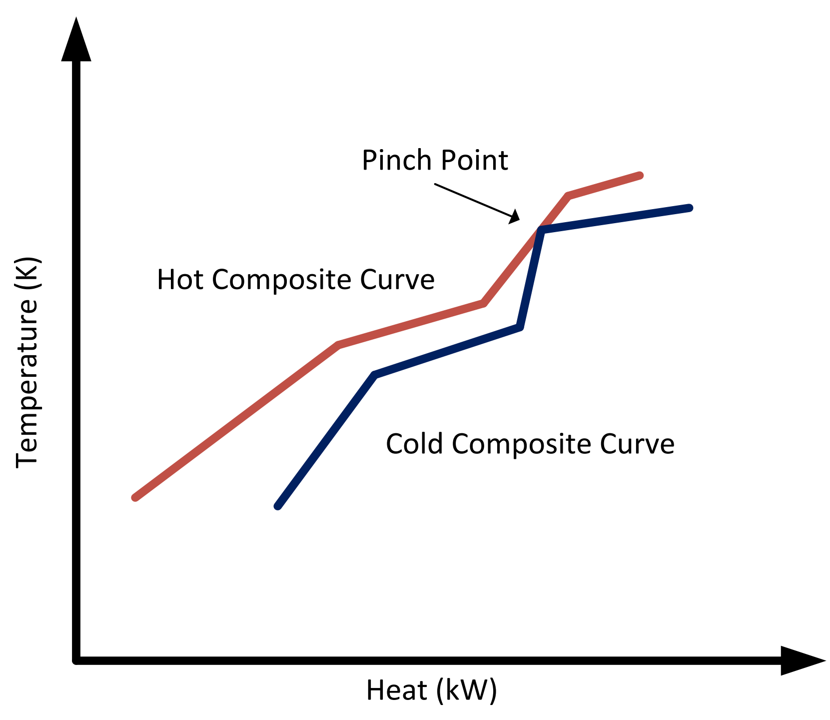


**Figure 5-Example of Composite Curve**

The composite curve allows the designer to determine where heat can be exchanged. Heat can only be transferred from one temperature to a lower temperature. This is important in using the composite curves as it can be determined where the transfer of heat is infeasible.

In some composite curves, there is a point known as a pinch point. The pinch point is where there is a minimum difference between the hot and cold composite curves. The pinch point is an important feature on the composite curve as that controls how much heat can be recovered. The use of the pinch point will be important in this work as it limits the amount of heat that can be transferred from the waste heat stream to the thermodynamic cycles.

### 3.5 Targeting

Targeting is a method used in process integration to determine how much of a certain utility is needed. For example, in heat integration, the objective of heat integration is to use hot streams to heat up streams that require heating. This allows for proper allocation of already available resources. If there are streams that require to be cooled using utilities, the amount of cooling required is known as the Cold Utilities target.  Ideally, this target is the minimum amount of cooling needed in the plant.

In the case of this work, a power target will be developed. This will be the maximum amount of power that can be generated from a set of waste heat streams. As in the case of other targets, this is an ideal target. This means that the amount of power that can be generated will always be less than the target due to efficiency losses. Two targets will be developed in this work; one target will be determined through the use of Carnot cycles and another target will be determined using the Rankine cycles.

CHAPTER IV

# CARNOT CYCLE TARGETING

## 4.1 Introduction

In this chapter, a methodology will be developed that can be used to determine the maximum amount of power that can be generated from a set of waste heat streams. This methodology will use the Carnot cycle to generate power. As mentioned before, the Carnot cycle is the thermodynamic cycle with the highest efficiency. Therefore, the target from this method will be the maximum amount of power that can be generated. A method to target power generation has not been developed and this methodology will allow for a designer to determine the maximum amount of power that can be generated. By using this method, it will allow designers to design towards a target. This methodology will be illustrated using case studies.

## 4.2 Problem Statement and Basic Relationships

The problem addressed in this work is formally stated as follows. Given is a set of hot streams that eject excess heat into the ambient. The composite T-H profile of these streams is available in the form of a hot composite curve developed using standard heat integration approaches described in Smith [7]. The composite T-H profile (Figure 6) has multiple segments, one in each temperature interval. The objective is to develop a simple algebraic procedure to determine the thermodynamic limit on the amount of power that can be generated from this profile.

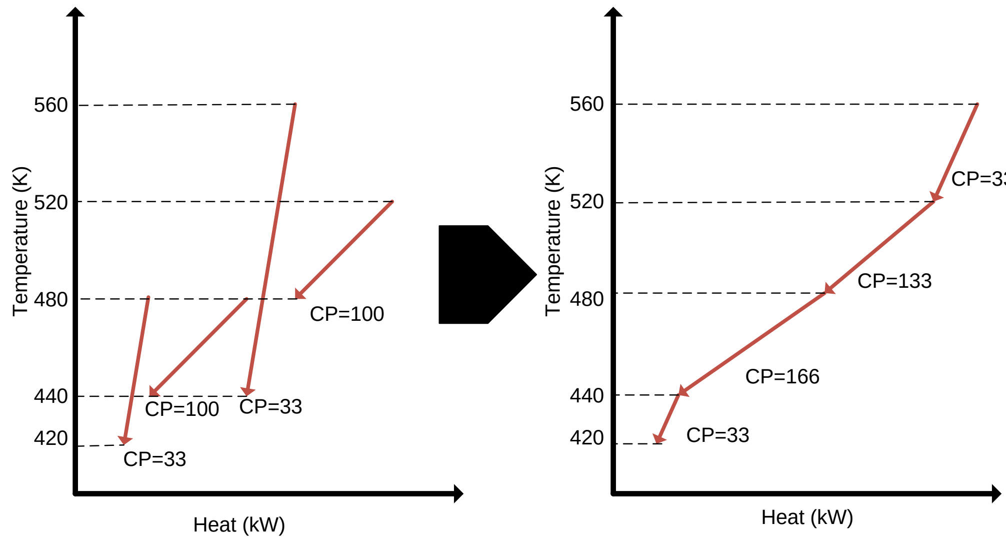


**Figure 6-Composite Curve for Multiple Hot Streams**

The most efficient thermal power generation process is the Carnot cycle, which is a basic element of this work and will be used to determine the maximum theoretical power generation from the heat sources. The Carnot cycle consists of four mechanically reversible steps, i.e. isothermal heat addition from a heat source at temperature $T_H$, isentropic expansion, isothermal heat removal into a heat sink at temperature $T_L$, and isentropic compression. In order for power to be generated in the cycle, $T_H$ needs to be greater than $T_L$. The Carnot cycle assumes that there is no energy lost due to friction, no exchange of heat between various parts of the engine, and heat transfers only from the heat source to the heat sink. The efficiency of the Carnot cycle can be calculated as

$$\eta = 1 - \frac{T_L}{T_H} \tag{3}$$

In the problem addressed in this work, heat is transferred from a composite heat source profile through Carnot cycles to a low temperature reservoir. In a given temperature interval from $T_i$ to $T_{i+1}$, the heat available from the source profile segment is given by

$$Q_j = CP_j(T_i - T_{i+1}) \quad (4)$$

$$Q_j = H_{v,j} \quad (5)$$

Equation 4 is applied for non-isothermal intervals where $CP_j$ is the heat capacity flowrate at constant pressure [kW/K] of the profile segment, $T_i$ is the inlet temperature [K] and $T_{i+1}$ is the exit temperature [K] of the heat source composite after heat has been removed. Equation 5 is applied for isothermal intervals where $H_{v,j}$ is the latent heat [kW]. For maximum power generation, the low temperature reservoir is assumed to be an isothermal utility at ambient temperature (TL) with an infinite heat capacity flow rate. The heat capacity is assumed to be constant due to relatively small variations over typical temperature ranges. In addition, the pressure drop within the stream is assumed to be zero.

While the Carnot cycle assumes the heat source to be isothermal, a typical heat source composite segment is not isothermal. As a result, for a single Carnot cycle, the hot reservoir would take the lowest source temperature in the temperature interval as illustrated in Figure 7, i.e. $T_H = T_{i+1}$.

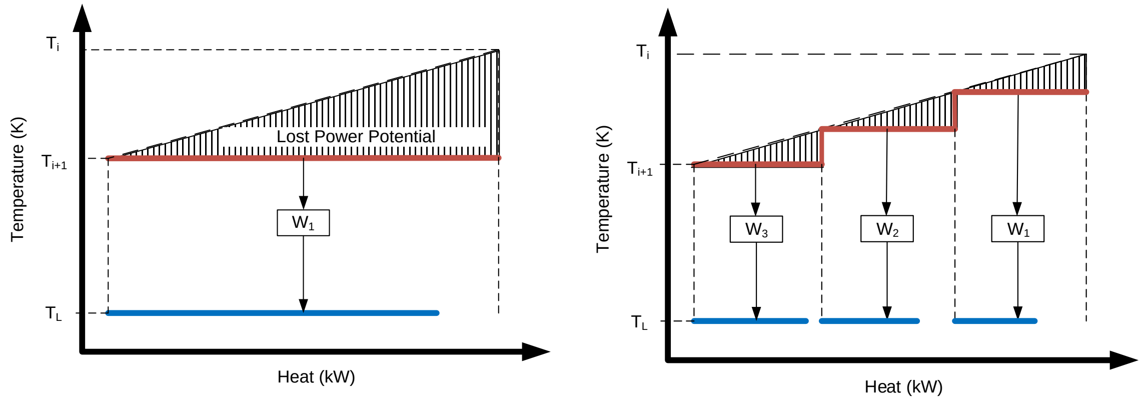


**Figure 7-Lost Power Potential Due to Single Carnot Cycle**

This will forfeit power generation potential and therefore present a lost opportunity for power generation. In order to increase power generation from the heat source profile, multiple Carnot cycles can be used as illustrated in Figure 8.

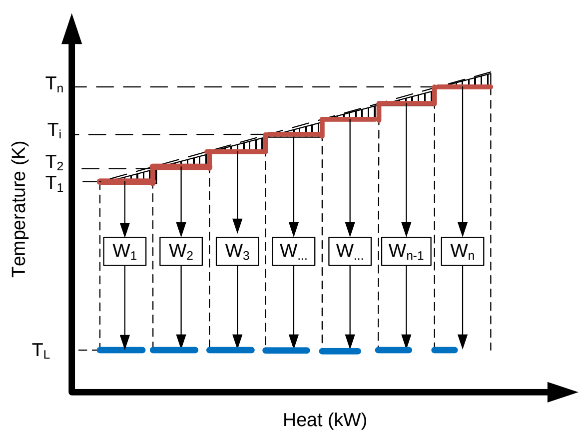


**Figure 8-Power Generation Using Multiple Carnot Cycles**

Using the area in between $T_i$ and $T_{i+1}$, the equation for heat can be derived as follows:

$$\Delta Q_j = CP_j \Delta T = CP_j (T_{i+1} - T_i) \tag{6}$$

In addition, the equation for the efficiency can be derived:

$$\eta_j = 1 - \frac{T_L}{T} = 1 - \frac{T_L}{T_i} \tag{7}$$

From the equations for heat and efficiency, the equation for power generated from $T_i$ to $T_{i+1}$ can be derived:

$$W_j = \eta_j \Delta Q_j = CP_j(T_{i+1} - T_i)\left(1 - \frac{T_L}{T_i}\right) \tag{8}$$

The total amount of work will be the following:

$$W_T = \sum_{i=1}^{n} W_i = \sum_{i=1}^{n} CP_j(T_{i+1} - T_i)\left(1 - \frac{T_L}{T_i}\right) \tag{9}$$

As the numbers of cycles approaches infinity, the hot temperature reservoirs of the Carnot cycles will approach the heat source profile and power generation will be maximized.

Over an infinitesimal temperature difference, the power that can be generated with a Carnot cycle is

$$dW = \eta dQ = CP_j\left(1 - \frac{T_L}{T}\right)dT \tag{10}$$

The maximum amount of power from a generated from a non-isothermal heat source composite segment is determined via integration over the temperature range of the interval from $T_{i+1}$ to $T_i$

$$W_j^{max} = \int dW = \int_{T_{i+1}}^{T_i} CP_j \left(1 - \frac{T_L}{T}\right) dT \tag{11}$$

The analytical solution of Equation 12 is given by

$$W_j^{max} = CP_j(T_i - T_{i+1}) - CP_j\, T_L \left[\ln\left(\frac{T_i}{T_{i+1}}\right)\right] \tag{12}$$

For the special case of an isothermal interval with $T_{i+1} = T_i$, the maximum work becomes:

$$W_j^{max} = H_{v,j}\left(1 - \frac{T_L}{T_i}\right) \tag{13}$$

Equation 12 is also known as availability. An alternative derivation of the equation is presented in the Appendix. Since heat flows are given from the T-H profiles and power generation needs to be determined, it is convenient to develop expressions for temperature interval power generation efficiencies. The efficiency for a non-isothermal interval and an isothermal interval are given by Equations 14 and 15:

$$\eta_j^{max} = \frac{W_j^{max}}{Q_j} = \frac{CP(T_i - T_{i+1}) - CPT_L\left[\ln\left(\frac{T_i}{T_{i+1}}\right)\right]}{CP(T_i - T_{i+1})} = 1 - \frac{T_L\left[\ln\left(\frac{T_i}{T_{i+1}}\right)\right]}{(T_i - T_{i+1})} \tag{14}$$

$$\eta_j^{max} = \frac{H_{v,j}\left(1 - \frac{T_L}{T_i}\right)}{H_{v,j}} = 1 - \frac{T_L}{T_i} \tag{15}$$

If the heat capacity needs to be expressed as a function of temperature, numerical integration of Equation 11 can be performed to determine the maximum amount of power that can be generated from an interval.

### 4.3 Algebraic Targeting Approach

This section presents an algebraic procedure to calculate the maximum amount of power generated from a heat source profile comprised of multiple streams. The procedure takes the form of a problem table algorithm and is similar in structure to approaches available for heat integration [7]. The maximum power generation can be quickly determined with the procedure, which involves only a few very quick calculations and can easily be completed in a spreadsheet.

The problem table is constructed from high to low temperature and considers each temperature interval of the problem as a row. Temperature intervals are determined from the T-H composite profile (Figure 6). Starting from the highest temperature and moving towards lower temperatures, the first temperature interval ends and the next interval starts, when a change in the slope of the composite occurs, i.e. a change in the presence of individual streams that comprise the composite segments occurs. The intervals are traced until the lowest temperature of the T-H composite is reached. In terms of temperature data, the start/end temperature of each interval is recorded in the problem table. Figure 9 shows a schematic of a basic problem table in its general form with N temperature intervals corresponding to N+1 temperature values. Each temperature interval is a row in the problem table, for which the following information is determined:

(a) The heat transferred from the hot streams (or composite) present in the interval into the cycle, which is determined using Equation 4 in the case of a non-isothermal interval, or using Equation 5 in the case of an isothermal interval.

(b) The interval power generation efficiency, which is determined using Equation 14 in the case of a non-isothermal interval, or using Equation 15 in the case of an isothermal interval.

(c) The maximum amount of power that can be generated from the heat available in the interval is determined as the product of available heat from (a) and interval power generation efficiency from (b).

| Interval | T (K) | $Q_{Interval}$ (kW) | $\eta_{Interval}$ (%) | $W_{Interval}$ (kW) |
|---|---|---|---|---|
| | $T_1$ | | | |
| 1 | | $Q_1$ | $\eta_1$ | $W_1=Q_1\eta_1$ |
| | $T_i$ | | | |
| i | | $Q_i$ | $\eta_i$ | $W_i=Q_i\eta_i$ |
| | $T_{i+1}$ | | | |
| i+1 | | $Q_{i+1}$ | $\eta_{i+1}$ | $W_{i+1}=Q_{i+1}\eta_{i+1}$ |
| | $T_{...}$ | | | |
| ... | | $Q_{...}$ | $\eta_{...}$ | $W_{...}=Q_{...}\eta_{...}$ |
| | $T_{N-1}$ | | | |
| N | | $Q_N$ | $\eta_N$ | $W_N=Q_N\eta_N$ |
| | $T_N$ | | | |
| System Totals | | $Q_T=\sum_{i=1}^{N} Q_i$ | $\eta_T = \frac{W_T}{Q_T}$ | $W_T = \sum_{i=1}^{N} W_i$ |

**Figure 9-Example Problem Table**

The calculations are performed for all temperature intervals, yielding the maximum power that can be generated from each interval hot stream composite segment. The total amount of power for the entire set of streams comprising the composite is obtained as the sum of power generation over all intervals.

Finally, we calculate the overall maximum theoretical (Carnot) efficiency of power generation from the set of heat source streams represented in the hot composite, i.e. over all N temperature intervals, as follows:

$$\eta_{sys}^{max} = \frac{\sum_{j=1}^{N} W_{max,j}}{\sum_{j=1}^{N} Q_j} \tag{16}$$

The cooling duty of the problem, i.e. the heat ejected from the hot streams for the initial case of no power generation, is reduced by the amount of power generated. This information may be useful to a designer interested in estimating possible reductions in cooling related footprints, e.g. cooling tower makeups or thermal pollution from marine discharges.

**4.4 Illustrative Examples**

The targeting procedure is illustrated with three example cases, for which the hot composite curves are shown in Figure 10. The data for the individual streams that make up the hot composites are summarized in Table 2. The temperature of the low temperature reservoir is assumed to be 298 K for all cases. The total amount of heat that needs to be removed from the hot streams is identical for all three cases (13,700 kW). Similarly, the streams in all three cases operate within the same temperature range. This means that a single Carnot cycle with a hot reservoir temperature at the lower temperature of the range (350 K), would have an efficiency of 14.9 % and produce the same amount of power (2035 kW) for all three cases.

The problem table for each case was developed using the procedure outlined in the previous section. The problem table for Case 1 is shown in Figure 11. As can be seen from the data and composite curve for Case 1 (Table 2 and Figure 11), there are three changes in the streams that comprise the composite, resulting in three temperature intervals. All temperature intervals are non-isothermal and the heat removed from the composites is determined from Equation 4 for all three intervals. For instance, in the second interval, the combined heat capacity flow rate of the composite segment comprised by streams 1 and 2 is 16 kW/K and the interval ranges from 560 K to 490 K, i.e. has an interval temperature difference of 70 K. This results in a combined heat removal from the hot streams in the interval to be 1,120 kW.

**Table 2- Streams Used for Carnot Cycle Illustrative Case Study**

| Example | Stream | CP (kW/K) | $T_{in}$ (K) | $T_{out}$ (K) | Q (kW) |
|---|---|---|---|---|---|
| Case 1 | Stream 1-1 | 7 | 560 | 350 | 1470 |
| | Stream 1-2 | 9 | 560 | 490 | 630 |
| | Stream 1-3 | 290 | 600 | 560 | 11600 |
| Case 2 | Stream 2-1 | ∞ | 500 | 500 | 6700 |
| | Stream 2-2 | 10 | 500 | 350 | 1500 |
| | Stream 2-3 | 15 | 560 | 500 | 900 |
| | Stream 2-4 | 10 | 600 | 500 | 1000 |
| | Stream 2-5 | 90 | 600 | 560 | 3600 |
| Case 3 | Stream 3-1 | ∞ | 450 | 450 | 6300 |
| | Stream 3-2 | 20 | 450 | 350 | 2000 |
| | Stream 3-3 | 30 | 400 | 350 | 1500 |
| | Stream 3-4 | 26 | 600 | 450 | 3900 |

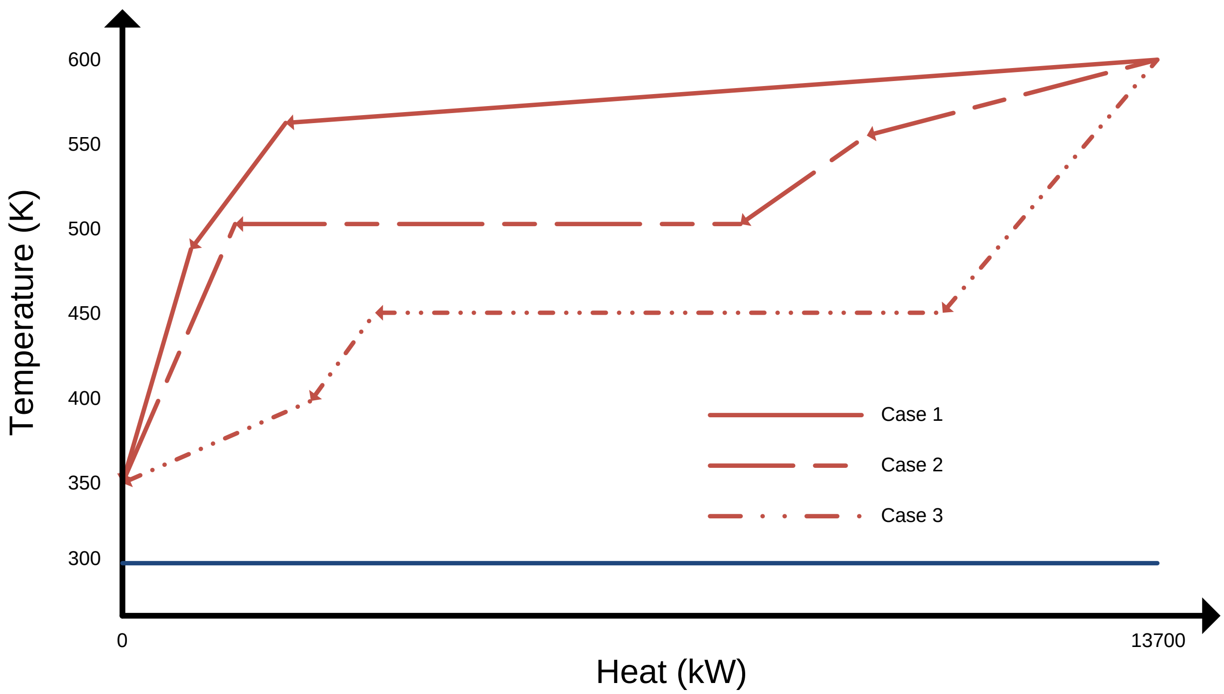


**Figure 10-Composite Curve for Carnot Cycle Illustrative Case Study**

Next, the interval efficiency for the non-isothermal interval is determined from Equation 17 using the interval temperatures:

$$\eta_2^{max} = 1 - \frac{298K\left[\ln\left(\frac{560K}{490K}\right)\right]}{(560K - 490K)} = 0.432 \tag{17}$$

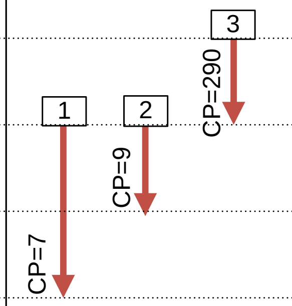


| Interval Temperature (K) | Stream Population | $\Delta T_{Interval}$ (K) | $CP_{Interval}$ (kW/K) | $Q_{Interval}$ (kW) | $\eta_{Interval}$ (%) | $W_{Interval}$ (kW) |
|---|---|---|---|---|---|---|
| 600 | | | | | | |
| | | 40 | 290 | 11600 | 48.6 | 5638 |
| 560 | | | | | | |
| | | 70 | 16 | 1120 | 43.2 | 483 |
| 490 | | | | | | |
| | | 140 | 7 | 980 | 28.4 | 278 |
| 350 | | | | | | |
| System Totals | | | | 13700 | 46.7 | 6399 |

**Figure 11-Problem Table for Carnot Cycle Case Study 1**

The resulting maximum power generation potential from the heat in the interval is found to be 483 kW. These calculations are repeated for each interval and the totals are determined. Over all three intervals, Case 1 has the potential to produce a maximum of 6,399 kW of power from the 13,700 kW of heat ejected from the streams, which results in an overall maximum power generation efficiency of 46.7%.The problem tables for Cases 2 and 3 are developed accordingly and shown in Figures 11 and 12. The third temperature interval of Case 2 (Figure 12) and the second temperature interval of Case 3 (Figure 13) are isothermal with a heat capacity flowrate approaching infinity. The heat ejected from the hot streams in these intervals and the maximum power generation efficiency is determined using Equations 5 and 15 respectively. Comparing the three cases, Case 1 ejects most heat at higher temperatures (Figure 10), which results in the highest maximum theoretical work (6,399 kW), followed by Case 2 (5,744 kW) and Case 3 (4,607 kW). This highlights the importance of developing case specific targets that consider the temperature vs. heat removal profiles of the multiple heat sources associated with a given problem.

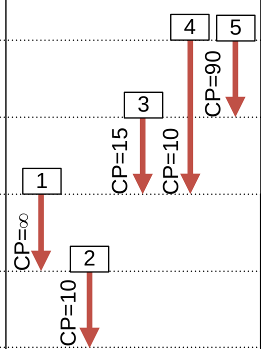


| Interval Temperature (K) | Stream Population | $\Delta T_{Interval}$ (K) | $CP_{Interval}$ (kW/K) | $Q_{Interval}$ (kW) | $\eta_{Interval}$ (%) | $W_{Interval}$ (kW) |
|---|---|---|---|---|---|---|
| 600 | | | | | | |
| | | 40 | 100 | 4000 | 48.6 | 1944 |
| 560 | | | | | | |
| | | 60 | 25 | 1500 | 43.7 | 656 |
| 500 | | | | | | |
| | | 0 | ∞ | 6700 | 40.4 | 2707 |
| 500 | | | | | | |
| | | 150 | 10 | 1500 | 29.1 | 437 |
| 350 | | | | | | |
| System Totals | | | | 13700 | 41.9 | 5744 |

**Figure 12-Problem Table for Carnot Cycle Case Study 2**

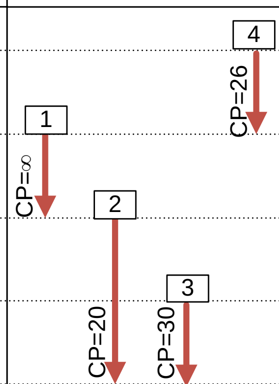


| Interval Temperature (K) | Stream Population | $\Delta T_{Interval}$ (K) | $CP_{Interval}$ (kW/K) | $Q_{Interval}$ (kW) | $\eta_{Interval}$ (%) | $W_{Interval}$ (kW) |
|---|---|---|---|---|---|---|
| 600 | | | | | | |
| | | 150 | 26 | 3900 | 42.8 | 1671 |
| 450 | | | | | | |
| | | 0 | ∞ | 6300 | 33.8 | 2128 |
| 450 | | | | | | |
| | | 50 | 20 | 1000 | 29.8 | 298 |
| 400 | | | | | | |
| | | 50 | 50 | 2500 | 20.4 | 510 |
| 350 | | | | | | |
| System Totals | | | | 13700 | 33.6 | 4607 |

**Figure 13-Problem Table for Carnot Cycle Case Study 3**

## 4.5 Comparison between Targeting Individual Streams and Composite Streams

The power generated by using the individual stream targeting technique and the composite stream targeting techniques will be compared. The power generated from both techniques should be the same. Case Study 3 will be used for this comparison. It was shown that the maximum amount of power that can be generated from Case Study 3 was 4607 kW. Using the equations mentioned earlier, the power for each individual stream will be calculated and the total amount of power generated from all of the streams will be determined.

The results for the stream-by-stream analysis is shown in Table 3.

**Table 3-Stream-by-Stream Analysis**

| Stream | CP (kW/K) | $T_i$ (K) | $T_f$ (K) | Q (kW) | Efficiency (%) | $W_{Stream}$(kW) |
|---|---|---|---|---|---|---|
| 1 | ∞ | 450 | 450 | 6300 | 33.8 | 2128 |
| 2 | 20 | 450 | 350 | 2000 | 25.1 | 502 |
| 3 | 30 | 400 | 350 | 1500 | 20.4 | 306 |
| 4 | 26 | 600 | 450 | 3900 | 42.8 | 1671 |
| Total | | | | 13700 | 33.6 | 4607 |

From this comparison, it can be seen that the maximum amount of power generated found from the stream-by-stream analysis and the composite analysis are the same. Therefore, either method can be used since the results will be the same. The method to use would depend on the designer's preference or the data availability.

The procedure can be used to determine the maximum power generation potential (target) from composites of multiple heat source streams quickly and reliably without the need for intensive calculations. All three cases of the illustrative examples, regardless of the number of temperature intervals involved, could be solved from scratch in MS Excel in a few minutes, which makes the procedure practical and attractive to develop maximum power generation potentials (targets) from excess (process) heat for use in high-level screening studies in line with the process integration philosophy of developing targets before design. Based on the targets, which represent the ideal case of maximum theoretical power, decisions can be taken to justify time for the development of specific power generation systems designs to generate power from the heat ejected from the multiple hot streams involved.

CHAPTER V

# RANKINE CYCLE TARGETING

## 5.1 Introduction

As in the previous chapter, the objective of this chapter is to develop a procedure that would determine the maximum amount of power that can be generated from waste heat streams. The previous chapter used the Carnot cycle to generate power. However, the Carnot cycle is not a real cycle that can be used to generate power. Therefore, an alternative power generating cycle needs to be used. The objective of this chapter is to develop a procedure that would determine the maximum amount of power that can be generated from waste heat streams using Rankine cycles. This method would allow for a better estimate than the Carnot targeting technique to determine how much power can be generated as it takes into account the preheating requirements and the minimum acceptable temperature difference.

## 5.2 Single Stream Matching Procedure

The objective of the single stream matching procedure is to determine the maximum amount of power that can be produced by Rankine cycles using heat from a single waste heat stream. The stream has a heat capacity flow rate, CP, initial temperature $T_s$, and final temperature $T_f$.

In order to demonstrate how heat will be transferred from the waste heat stream to the Rankine cycle, a composite curve will be used. The preheating and evaporation stages of the Rankine cycles will be represented by a cold composite curve. The waste heat stream will be represented by a hot composite curve. Using a composite curve will ensure that the heat transfer between the waste heat stream and the Rankine cycle is feasible. To develop a target for power generation using the Rankine cycle, heat must be converted into power at the highest efficiency possible. As a result, the Rankine cycle operating at the evaporation temperature with the highest efficiency, $T_{eff}$, should be used to extract heat from the waste heat streams.

The evaporation temperature of the first Rankine cycle system, $T_1$, depends on the initial temperature of the waste heat stream. It is not possible to use $T_s$ as the evaporation temperature so a lower temperature will need to be used. DT is the temperature size that will be used in this work. Ideally, the temperature step size should be infinitesimally small. The smaller the temperature step size, more Rankine cycles can be used and thus greater power generation. However, for computational purposes, the temperature step size used in this study will be in the range of .1 to 4 K. For the case in which $T_s$ is lower than $T_{eff}$, Equation 18 will be used. For the case in which $T_s$ is equal to or higher than $T_{eff}$, Equation 19 will be used.

$$T_1 = T_s - DT \qquad (18)$$

$$T_1 = T_{eff} \qquad (19)$$

It is important to note that not all of the heat from the waste heat stream can be extracted using the Rankine cycle operating at the evaporation temperature of $T_1$ due to the minimum acceptable temperature difference. There would be a possibility of infeasibility in the heat transfer between the waste heat stream and the working fluid as shown in

Figure 14. The infeasibility is a result of attempting to transfer heat from the Rankine cycle to the waste heat stream when the opposite should occur. As a result, the mass flow rate of the Rankine cycle must be limited such that there is a pinch point between the composite curves of the Rankine cycle and the waste heat stream.

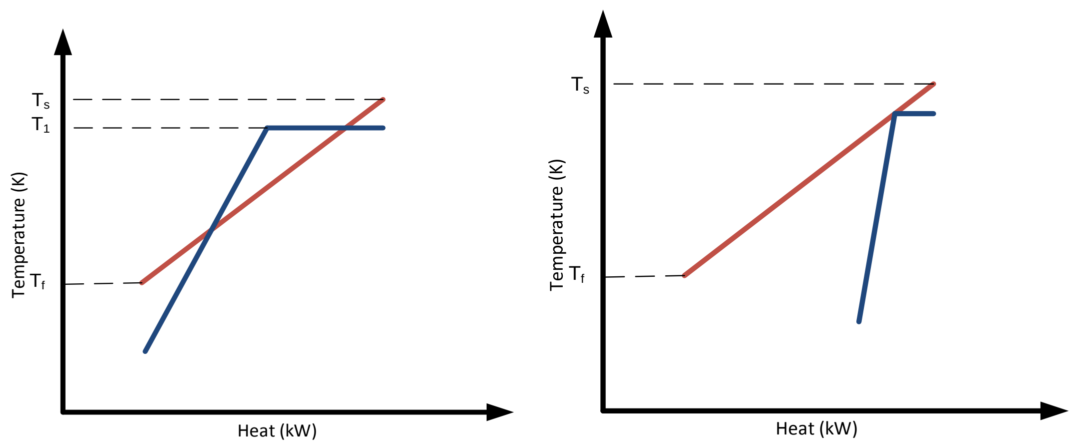


**Figure 14-Infeasible and Feasible Heat Transfer**

To avoid any infeasibility, the mass flow rate of the Rankine cycle will determined such that either a) a pinch point will occur between the composite curves or b) all of the heat from the waste heat stream will be used. As seen from Figure 14, one Rankine cycle will usually not be enough to utilize all of the heat from the waste heat stream.

The mass flow rate is calculated in order for the Rankine cycle to have a pinch point. The mass flow rate for the first evaporation temperature, $m_1$, can be found using the energy balance between the waste heat stream and the cycle. The heat transferred from the waste heat stream should be equal to the heat required for the evaporation of the working fluid in the Rankine cycle.

$$CP * DT = m_1(T_1)\left[h_2(T_1, P_{sat,1}) - h_1(T_1, P_{sat,1})\right] \tag{20}$$

As a result, the mass flow rate of the working fluid for the first Rankine cycle can be determined using Equation 21.

$$m_1(T_1) = \frac{CP * DT}{\left[h_2(T_1, P_{sat,1}) - h_1(T_1, P_{sat,1})\right]} \tag{21}$$

For a few special cases (including isothermal streams and where $T_1 = T_{eff}$), the energy balance is given in Equation 22.

$$Q = m[h_2(T, P) - h_5(T, P)] \tag{22}$$

From the energy balance, the mass flow rate can be determined as follows:

$$m = \frac{Q}{[h_2(T, P) - h_5(T, P)]} \tag{23}$$

There is a trade-off in selecting the evaporation temperature. A Rankine cycle with a higher evaporation temperature allows for high efficiencies, however a lower amount of heat would be used. Therefore, using a cycle with a high evaporation temperature does not guarantee maximum power, only maximum efficiency.

In order to guarantee maximum power, additional Rankine cycles need to be used in order to extract all of the heat from the heat source as shown in Figure 15.

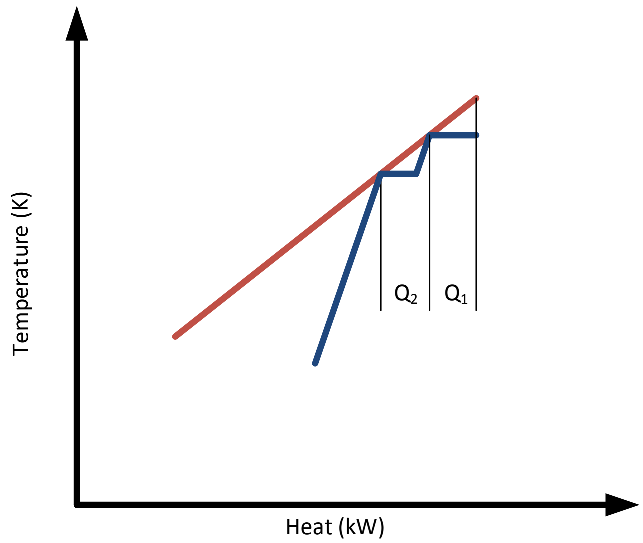


**Figure 15-Using Two Rankine Cycles**

Before deciding if another Rankine cycle should be added, an energy balance check needs to be done to ensure that not all of the heat available from the waste heat stream has been used. The heat balance between the waste heat stream and the Rankine cycle will be checked.

$$CP(T_s - T_f) = \sum_{i=1}^{n} m_i\left[h_2\left(T_i, P_{sat,i}\right) - h_5(T_i, P_{sat,i})\right] \tag{24}$$

$$CP(T_P - T_f) \leq m_n\left[h_1\left(T_P, P_{sat,i}\right) - h_5\left(T_P, P_{sat,i}\right)\right] + \sum_{i=1}^{n-1} m_i\left[h(T_P, P_{sat,i}) - h_5(T_i, P_{sat,i})\right] \tag{25}$$

If the energy balance is not satisfied, there are two possibilities; there is heat remaining that can be used or there is an infeasibility due to using heat that is not available. For the first case, this can be corrected by adding additional cycles. The second case only occurs when too many cycles have been used or if the mass flow rate of one of the cycles causes infeasibility.

Once the minimum acceptable temperature difference has been reached for the evaporation temperature, a Rankine cycle with a lower evaporation temperature will be used. The next temperature that will be used depends on the temperature step size, DT.

$$T_{i+1} = T_i - DT \tag{26}$$

The mass flow rate for the second Rankine cycle will also be determined using the energy balance equations. However, for the case of the second Rankine cycle, the energy balance includes the heat required for the evaporation of the working fluid for the current cycle and preheating needed for the first Rankine cycle.

The energy balance for the second evaporation temperature is shown in Equation 28.

$$Q_2 = CP * DT \tag{27}$$

$$m_2(T_2)\left[h_2\left(T_2, P_{sat,2}\right) - h_1\left(T_2, P_{sat,2}\right)\right] + m_1\left[h_1\left(T_1, P_{sat,1}\right) - h\left(T_1, P_{sat,1}\right)\right] = CP * DT \tag{28}$$

From the energy balance equation, the mass flow rate of the second Rankine cycle can be determined.

$$m_2(T_2) = \frac{CP * DT - m_1\left[h_1\left(T_1, P_{sat,1}\right) - h\left(T_1, P_{sat,1}\right)\right]}{\left[h_2\left(T_2, P_{sat,2}\right) - h_1\left(T_2, P_{sat,2}\right)\right]} \tag{29}$$

As with before, another Rankine cycle will be added if all of the heat has not been utilized. The energy balance for the third Rankine cycle includes the evaporation for the current cycle and the preheating of the previous two cycles. This is shown in Figure 16.

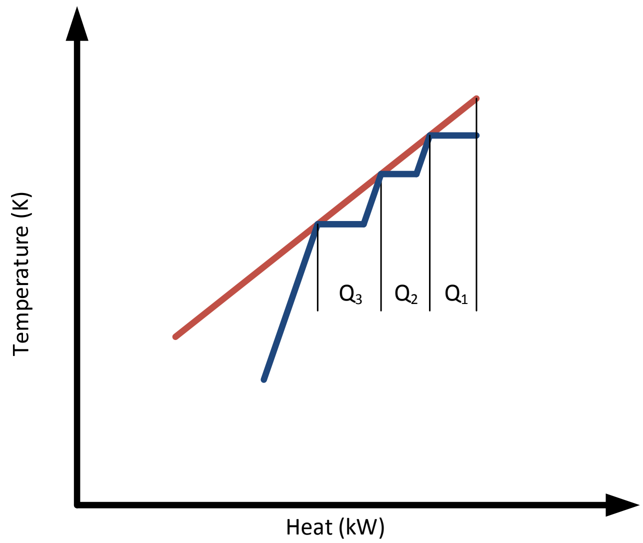


**Figure 16-Using Three Rankine Cycles**

$$m_3(T_3)\left[h_2\left(T_3, P_{sat,3}\right) - h_1\left(T_3, P_{sat,3}\right)\right] + m_2\left[h_1\left(T_2, P_{sat,2}\right) + h\left(T_3, P_{sat,2}\right)\right] + m_1\left[h\left(T_2, P_{sat,1}\right) - h\left(T_3, P_{sat,1}\right)\right] = CP * DT \tag{30}$$

The mass flow rate of the third Rankine cycle can be found using the heat balance.

$$m_3(T_3) = \frac{CP * DT - m_2\left[h_1\left(T_2, P_{sat,2}\right) + h\left(T_3, P_{sat,2}\right)\right] - m_1\left[h\left(T_2, P_{sat,1}\right) - h\left(T_3, P_{sat,1}\right)\right]}{\left[h_2\left(T_3, P_{sat,3}\right) - h_1\left(T_3, P_{sat,3}\right)\right]} \tag{31}$$

The generalization of the mass flow rate equation is shown in Equation 32.

$$m_i(T_i) = \frac{CP*DT - m_{i-1}\left[h_1\left(T_{i-1}, P_{sat,i-1}\right) - h\left(T_i, P_{sat,i-1}\right)\right] - \sum_{k=i-2}^{k=i-1} m_k\left[h\left(T_{k+1}, P_{sat,k}\right) - h\left(T_{k+1}, P_{sat,k}\right)\right]}{\left[h_2\left(T_i, P_{sat,i}\right) - h_1\left(T_i, P_{sat,i}\right)\right]}$$

(32)

The procedure will be repeated until all of the heat from the waste heat stream is used. The final Rankine cycle operates at the operating temperature, $T_{min}$, and is identifiable on the composite curve. Figure 17 shows the cold composite curve once the matching procedure has been completed. The flowchart for the procedure is shown in Figure 18.

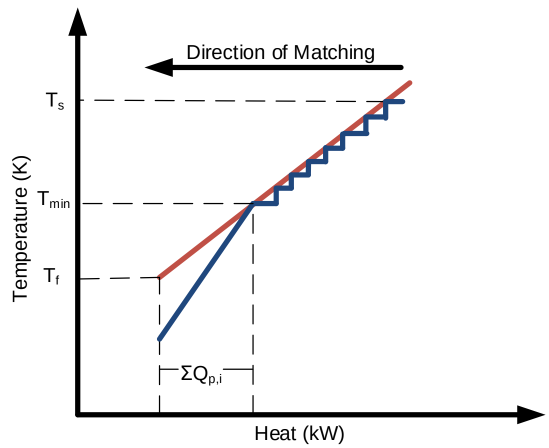


**Figure 17- Multiple Rankine Cycles Using Available Heat**

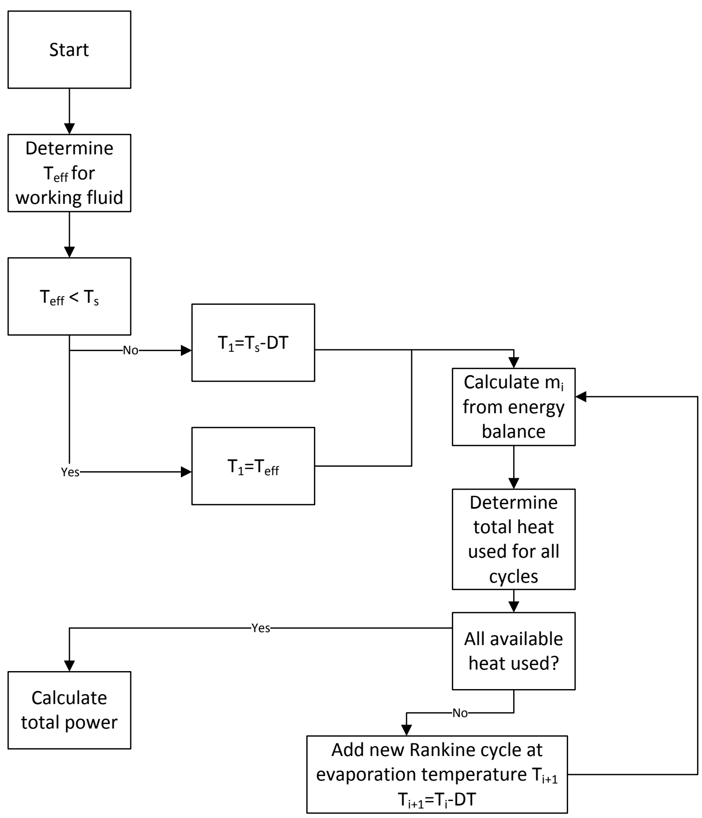


**Figure 18-Flowchart for Matching Procedure**

As a result of this procedure, the mass flow rate of the working fluid for each cycle can be determined. The composite curves for the Rankine cycles generated after the procedure can be drawn as in Figure 19. The horizontal lines in the cold composite curve represent the evaporation stages of the Rankine cycle and the sloped lines represent the preheater stages. As a result, the cold composite curve will be in a staircase shape as there are multiple Rankine Cycles with preheating stages in between each evaporation temperature.

The matching is done in two directions. The first direction is from higher temperatures to lower temperatures (or top to bottom). The matching is done from top to bottom in order to ensure that the cycles used are those that generate power at the highest efficiencies. As the mass flow rate of a cycle is limited by the amount of heat available at certain temperatures, it is not possible to use one cycle. After using all of the heat possible for one cycle, another cycle needs to be used. As the goal is to generate as much power as possible, the next cycle to be used is the cycle with the next highest efficiency. This means that another evaporation temperature needs to be selected that is less than the previous evaporation temperature. Therefore, there are multiple cycles that operate at different evaporation temperatures.

Matching is also done from right to left. In order to make sure that there is enough heat for the cycles with the higher temperatures, the availability of heat at the required temperatures is checked. This is done by using the energy balance between the waste heat stream and the Rankine cycles to ensure the amount of heat being exchanged is equal.

The purpose of the matching procedure is to determine that heat is available at the required temperature while producing power at the highest efficiency possible. The mass flow rate of the working fluid for each cycle is determined from the procedure. Once the mass flow rates for each cycle have been determined, the power produced from each cycle can be easily determined.

The circled portion of the cold composite curve in Figure 19 is where preheating for all of the cycles is done. The figure shows that the preheating is done from the minimum temperature of the cycles to $T_{min}$. The cycles at the higher temperatures need to be preheated at temperatures higher than $T_{min}$.

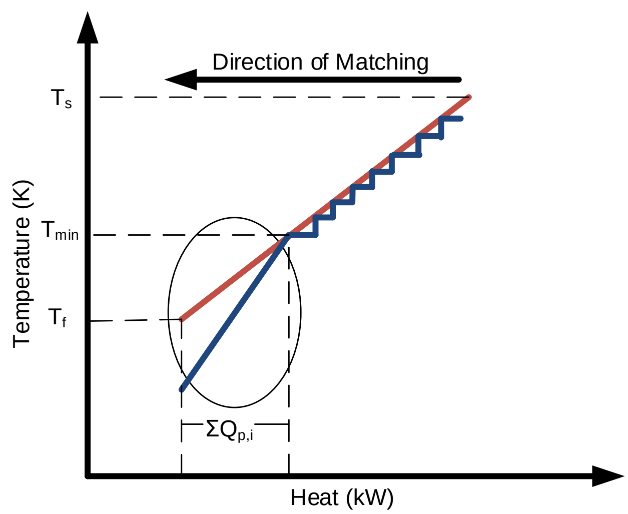


**Figure 19-Preheating of All Rankine Cycles**

The preheating for the higher temperatures and the evaporation is done in the circled portion of the cold composite curve in Figure 20. The preheating done in these "steps" is the preheating required for all of the cycles at higher temperatures. The flat lines are the heating done for the evaporation of the working fluids.

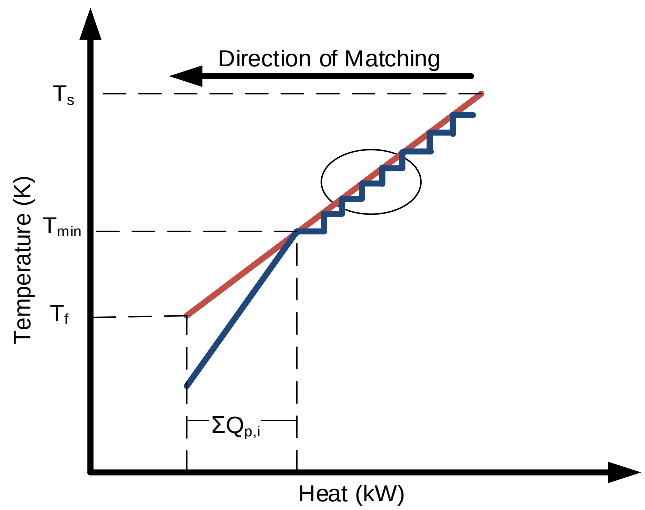


**Figure 20-Evaporating and Preheating of Rankine Cycles**

Once the mass flow rate of the working fluid for each cycle is found, the amount of power generated can be determined from the Equation 33:

$$W_{max} = \sum_{i=1}^{n} W_i = \sum_{i=1}^{n} Q_i \eta_i = \sum_{i=1}^{n} m_i \left[h_2\left(T_i, P_{sat,i}\right) - h_5\left(T_i, P_{sat,i}\right)\right] \eta_i \tag{33}$$

The efficiency of the system can be determined using Equation 34.

$$\eta_{single} = \frac{W_{max}}{Q} = \frac{W_{max}}{CP(T_s - T_f)} \tag{34}$$

### 5.3 Individual Stream Targeting Illustrative Case Study

The individual stream targeting methodology will be demonstrated using different streams. The stream data that will be used in this case study is in Table 4. The objective of this case study is to determine the maximum amount of power that can be generated from Rankine cycles using benzene as their working fluid. It is expected that power generation target would be less than that from the Carnot targeting method. The methodology was implemented in MATLAB using the code in Appendix B.

**Table 4- Rankine Targeting Case Study Streams**

| Stream | CP (kW/K) | $T_s$ (K) | $T_f$ (K) | Q (kW) |
|---|---|---|---|---|
| 1 | 10 | 600 | 400 | 2000 |
| 2 | 40 | 500 | 400 | 4000 |
| 3 | 70 | 460 | 350 | 7700 |

The single stream matching procedure was used to determine the maximum theoretical amount of power that could be generated from the streams in Table 4. The temperature step size used was 1 K. The results from the matching procedure are in Table 5.

**Table 5- Individual Stream Targeting Results**

| Stream | CP (kW/K) | $T_s$ (K) | $T_f$(K) | $Q_t$ (kW) | $T_{min}$ (K) | W (kW) | Efficiency (%) |
|---|---|---|---|---|---|---|---|
| 1 | 10 | 600 | 400 | 2000 | 557 | 665.51 | 33.28 |
| 2 | 40 | 500 | 400 | 4000 | 446 | 1142.23 | 28.56 |
| 3 | 70 | 460 | 350 | 7700 | 379 | 1857.12 | 24.12 |
| Total | | | | 13700 | | 3664.86 | 26.75 |

Similar to the Carnot targeting method, the efficiencies are highest for those streams that are at higher temperatures. Stream 1 has a greater efficiency than the other two streams as it starts at a higher temperature. Because Stream 1 has a starting temperature greater than $T_{eff}$, only on Rankine cycle will be used at the evaporation temperature $T_{eff}$. As a result, all of the heat is converted to power at the efficiency of 33.33 %. The composite curves for Stream 1 can be seen in Figure 21.

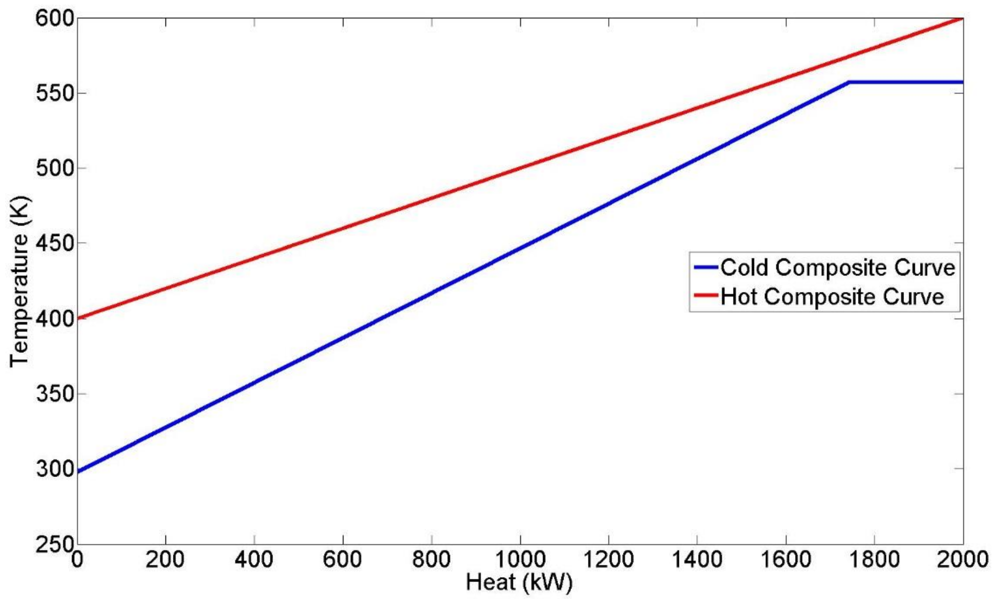


**Figure 21-Individual Stream Matching for Stream 1**

For the cases of Stream 2 and 3, their starting temperatures is less than $T_{eff}$ therefore the first evaporation temperature will be at the starting temperature of the waste heat stream. This is shown in Figure 22 for the case of Stream 2. Power is generated starting from the highest temperature until all of the heat is used. For the case of Stream 2, the final evaporation temperature was 446 K.

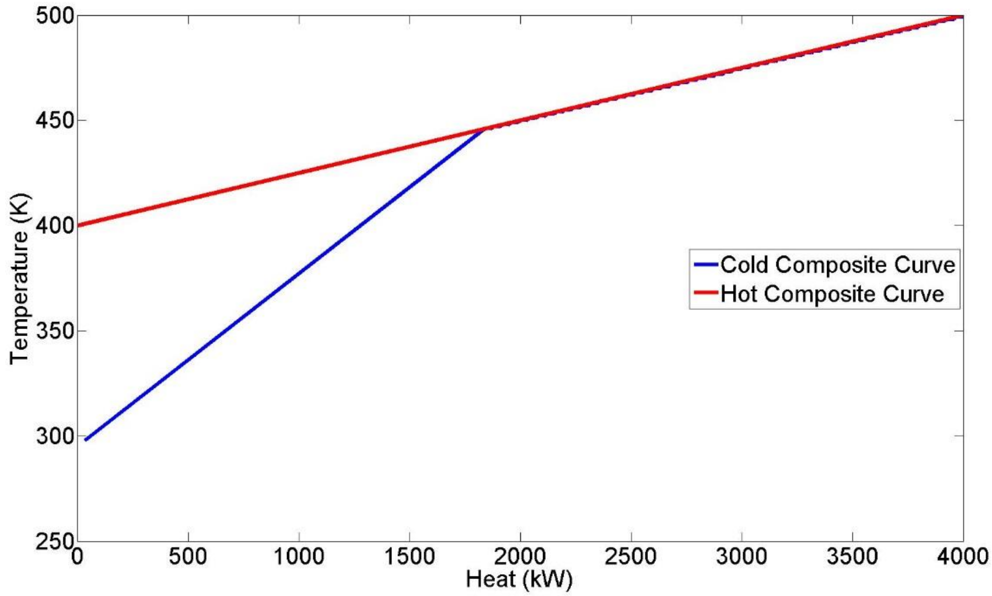


**Figure 22-Individual Stream Matching for Stream 2**

A comparison between the power generated from the Carnot targeting method and the Rankine targeting method is in Table 6.

**Table 6- Comparison between Carnot Cycle Targeting and Rankine Cycle Targeting**

| Stream | RC Power (kW) | Carnot Power (kW) | RC Efficiency (%) | Carnot Efficiency (%) |
|---|---|---|---|---|
| 1 | 665.51 | 791.71 | 33.28 | 39.59 |
| 2 | 1142.23 | 1340.13 | 28.56 | 33.50 |
| 3 | 1857.12 | 1999.10 | 24.12 | 25.96 |

As discussed previously, the target from the Carnot targeting procedure is the maximum amount of power that can be generated. Therefore, it is expected that the amount of power generated from the Rankine cycles targeting procedure would be less than the power generate by the Carnot targeting procedure. The difference in efficiency between the Rankine cycle efficiency and the Carnot efficiency range from 1-6%. There is a significant difference between the efficiencies for Stream 1. This is a result of the initial temperature being higher than $T_{eff}$ for benzene.

### 5.4 Multiple Stream Matching Procedure

For the case in which multiple waste heat streams are available, targeting can be done in a similar procedure as the single waste heat stream. Before the matching procedure can be started, the hot composite curve for the waste heat streams should be drawn.

The objective of this multiple stream matching procedure is the same as the previous section; to determine the mass flow rate of the working fluid for each Rankine cycle. The multiple stream matching procedure is similar to that of the single stream matching, however there are a few differences as the heat capacity flow rate changes with temperature.

As with before, the first step is to determine the initial evaporation temperature. This depends on the highest temperature of the hot composite curve. If the highest temperature of the hot composite curve is less than $T_{eff}$, the initial evaporation temperature will be the highest temperature of the hot composite curve. If the highest temperature of the hot composite curve is greater than $T_{eff}$, the initial evaporation temperature will be Teff.

The initial evaporation temperature will be found using Equations 35 and 36

$$T_1 = T_s - DT \tag{35}$$

$$T_1 = T_{eff} \tag{36}$$

The next step is to determine the mass flow rate of the working fluid at the first evaporation temperature. The mass flow rate of the first evaporation temperature can be found using the following equation.

This is unlike the equation used for the single stream matching. The reason for this is that infeasibility can occur. To determine the mass flow rate, the heat capacity flow rate of the next interval needs to be considered.

$$m_i(T_i) = \frac{CP(T_i)dT - m_{i-1}[h_1(T_{i-1}, P_{sat,i-1}) - h(T_i, P_{sat,i-1})] - \sum_{k=i-2}^{k=i-1} m_k[h(T_{i-1}, P_{sat,k}) - h(T_i, P_{sat,k})]}{[h_2(T_i, P_{sat,i}) - h_1(T_i, P_{sat,i})]} \quad (37)$$

$$\int_{T_f}^{T_p} CP(T)dT \leq m_n\left[h_1(T_P, P_{sat,i}) - h_5(T_P, P_{sat,i})\right] + \sum_{i=1}^{n-1} m_i\left[h(T_P, P_{sat,i}) - h_5(T_i, P_{sat,i})\right] \quad (38)$$

$$\int_{T_f}^{T_s} CP(T)dT = \sum_{i=1}^{n} m_i\left[h_2(T_i, P_{sat,i}) - h_5(T_i, P_{sat,i})\right] \quad (39)$$

When the targeting procedure has been completed, the composite curve will be similar to the one shown in Figure 23.

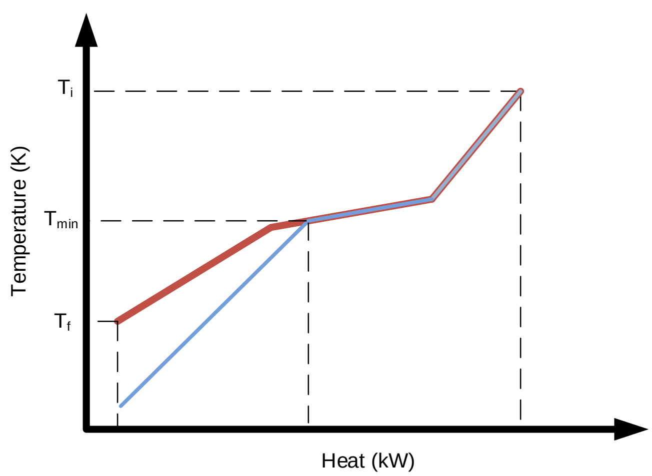


**Figure 23-Multiple Stream Matching Composite Curve**

The total amount of power generated can be calculated from Equation 40.

$$W_{max} = \sum_{i=1}^{n} W_i = \sum_{i=1}^{n} Q_i \eta_i = \sum_{i=1}^{n} m_i \left[h_2\left(T_i, P_{sat,i}\right) - h_5\left(T_i, P_{sat,i}\right)\right] \eta_i \qquad (40)$$

The efficiency of the system can be found using Equation 41.

$$\eta_{composite} = \frac{W_{max}}{Q} = \frac{W_{max}}{\int_{T_s}^{T_f} CP(T)dT} \qquad (41)$$

**5.5 Multiple Stream Illustrative Case Study**

The streams used for the single stream illustrative case study will be used for the multiple stream targeting. The temperature step size used was 1 K. The streams that will be used are found in Table 4. This case study will determine if the same results will be obtained from the multiple stream matching procedure and the individual stream matching.

The results for the targeting method are shown in Table 7.

**Table 7-Multiple Stream Targeting Results**

| Streams | $Q_t$ (kW) | $T_{min}$ (K) | W (kW) | Efficiency (%) |
|---|---|---|---|---|
| 1,2,3 | 13700 | 410 | 3810.18 | 27.81 |

The composite curve for the case study is shown in Figure 24. As the starting temperature of the composite curve is greater than Teff, the first evaporation temperature is at $T_{eff}$. This evaporation temperature is used until it reaches the pinch point at 500 K. The second evaporation temperature is 500 K and it continues to decrease by the temperature step size until the all of the heat has been used. The results from the targeting method show that an efficiency of 27.81 % can be achieved using Streams 1 through 3. This can be compared to the results of the total system efficiency from the individual stream targeting. The system efficiency of the multiple stream analysis, 27.81 %, is higher than that from the individual stream targeting, 26.75 %. This analysis shows that using the multiple stream analysis can generate results that are not possible from the individual targeting method.

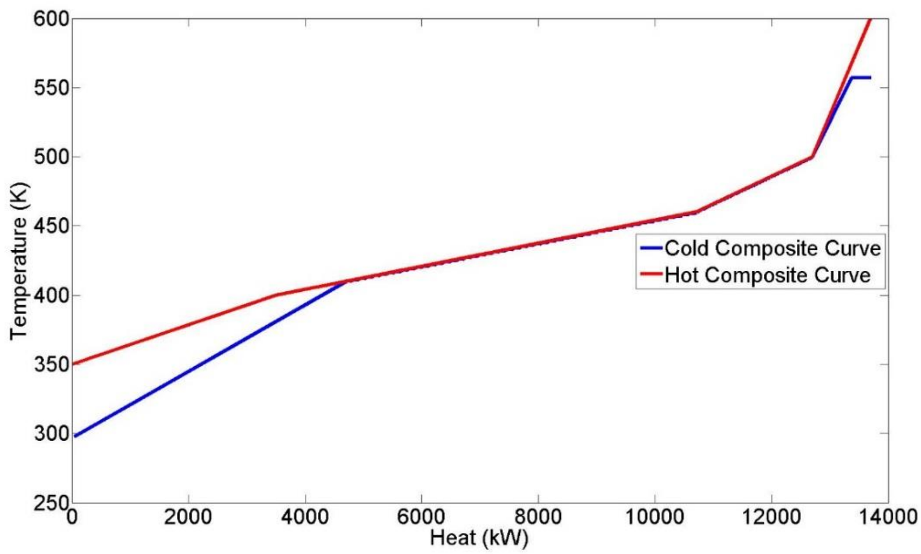


**Figure 24-Multiple Stream Matching of Case Study**

Power is generated at higher efficiencies from the multiple stream matching as the preheating can be done from the streams with lower temperatures. However, for the single streams, the preheating is done using the individual streams. This means that taking into account all of the streams leads to a higher power target. This will be looked at more in depth in the next section.

## 5.6 Comparison between Individual Stream Matching and Multiple Stream Matching

In the case studies, it was shown that the individual stream matching and the composite stream matching produced different results for the same streams. This leads to the following question: Why would the individual and multiple stream matching give two different results?

Three cases will be used to determine the difference between using the multiple stream matching and the individual stream matching. Table 8 shows the streams that will be used for the comparison. As mentioned, the three cases have different individual streams but identical composite curves.

**Table 8-Individual and Multiple Stream Cases**

| Case | Stream | CP (kW/K) | $T_s$(K) | $T_f$ (K) | Q (kW) |
|---|---|---|---|---|---|
| 1 | 1 | 10 | 500 | 450 | 500 |
| | 2 | 10 | 450 | 300 | 1500 |
| 2 | 3 | 10 | 500 | 400 | 1000 |
| | 4 | 10 | 400 | 300 | 1000 |
| 3 | 5 | 10 | 500 | 350 | 1500 |
| | 6 | 10 | 350 | 300 | 500 |

The individual stream matching procedure will be done for each individual stream and the maximum power generated from that analysis will be compared to the multiple stream analysis. It is important to note that each of the cases have the same composite curve, which is a stream with a heat capacity flow rate of 10 kW/K with a starting temperature of 500 K and a final temperature of 300 K. If the individual stream matching and the multiple stream matching give the same results, then each case should have the same amount of power generated and the results should be the same as that of the composite stream. Streams 1 and 2 are shown in Figure 25.

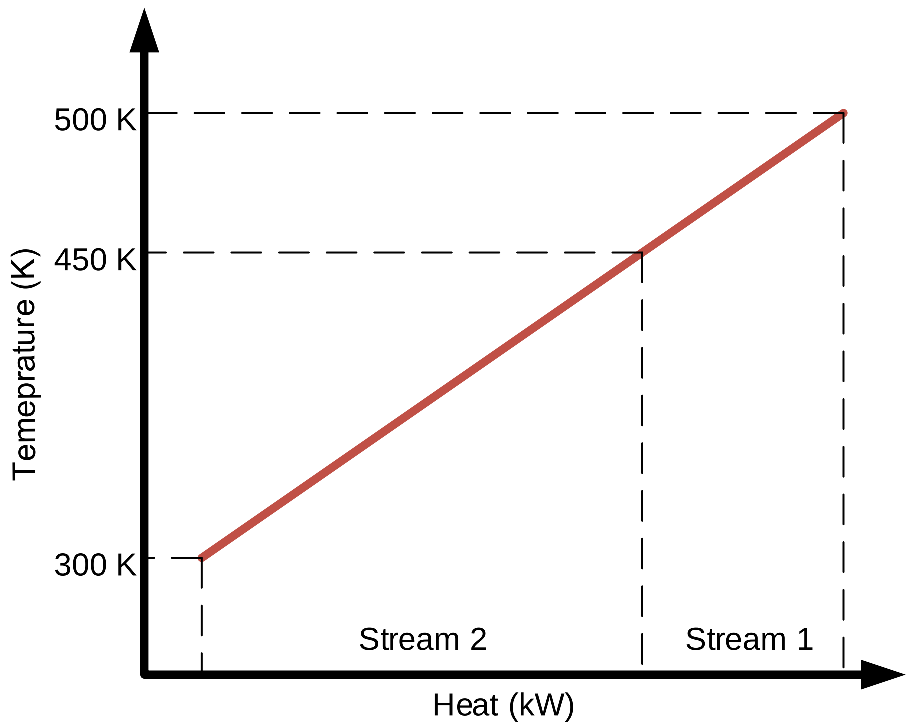


**Figure 25-Stream 1 and Stream 2 "Composite" Curve**

The power generated and the efficiency for each of the three cases is shown in Table 9.

**Table 9-Individual and Multiple Stream Cases Results**

| Case | Stream | Power (kW) | Efficiency (%) |
|---|---|---|---|
| 1 | 1 | 144.00 | 28.80 |
| | 2 | 291.55 | 19.44 |
| | Total | 435.55 | 21.78 |
| 2 | 3 | 285.55 | 28.56 |
| | 4 | 141.86 | 14.19 |
| | Total | 427.41 | 21.37 |
| 3 | 5 | 409.00 | 27.27 |
| | 6 | 39.91 | 7.98 |
| | Total | 448.91 | 22.45 |

Each case has its own efficiency and power generated when the single stream matching procedure is done. The composite curve for the individual stream matching can be seen in Figure 26.

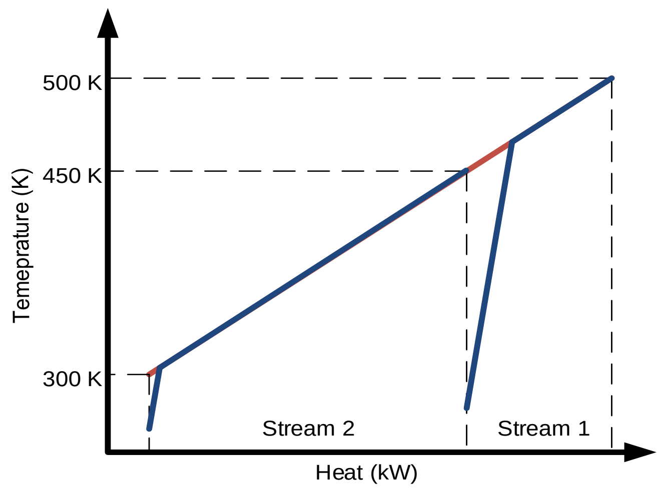


**Figure 26-Individual Stream Matching**

The composite curve shows that there are no Rankine cycles with evaporation temperatures from $T_{min}$ to 450 K. This would represent a significant amount of power loss since these temperatures are at the higher temperature range for these streams. More power would be produced if Rankine cycles were used in the mentioned temperature range. Instead of being used for evaporation, the heat at that temperature range is being used for preheating. As a result, it should be expected that the multiple stream matching will produce more power since there are Rankine cycles with evaporation temperatures between $T_{min}$ and 450 K. Table 10 shows the results for the composite stream matching for Streams 1 and 2. The composite curve for the composite stream matching is shown in Figure 27.

**Table 10-Results from Multiple Stream Matching**

| Stream | Power (kW) | Efficiency (%) |
|---|---|---|
| Composite | 478.67 | 23.93 |

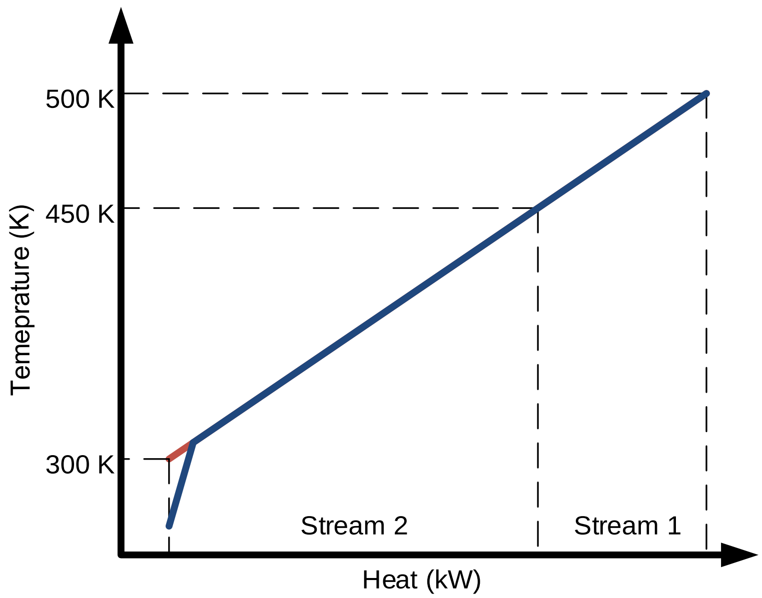


**Figure 27-Multiple Stream Matching**

As a result of this analysis, it was shown that using the multiple stream matching procedure results in higher efficiencies than using the individual steam matching procedure. Therefore, it is important to know all of the available streams when doing the multiple stream matching procedure. Otherwise, opportunities for higher efficiencies would be missed. The reason why the composite stream matching procedure would provide higher efficiencies is because the preheating is done at the lower temperatures. This allows for power to be generated at higher temperatures.

This is unlike the Carnot targeting where the results from the composite analysis and the individual stream analysis were the same. As a result, in order to determine the maximum amount of power that can be generated from a given set of streams, the multiple stream matching procedure should be used.

### 5.7 Effect of Step Size on $W_{max}$

By decreasing the step size, a greater number of Rankine cycles will be used. This would increase the efficiency of the system as Rankine cycles have higher efficiencies at higher temperatures. By decreasing the step size, more power will be generated and will result in a higher target. Ideally, the temperature step size would be infinitesimally small. In this study, the minimum step size that will be used is .1 K.

A study was done to see the effect of decreasing the step size on the amount of power generated. The amount of power generated will increase as the step size decreases. The reason for this is that power will be generated at more evaporation temperatures with higher efficiencies. The results are shown in Table 11.

**Table 11-Effect of Step Size on Power Generated**

| Step Size (K) | Power (kW) | Efficiency (%) |
|---|---|---|
| .1 | 1164.28 | 29.11 |
| 1 | 1142.23 | 28.56 |
| 2 | 1127.99 | 28.20 |
| 4 | 1070.22 | 26.76 |

As a result of this work, a methodology to determine the maximum amount of power generated from a given set of waste heat stream using Rankine cycles has been developed. An important conclusion from this chapter is that the composite stream matching procedure should be used when more than one stream is available. This is unlike the Carnot targeting procedure.

# CHAPTER VI

## SUMMARY AND CONCLUSIONS

The objective of this work was to determine power generation targets from waste heat streams. This allows designers to quickly determine if it is worth going into detailed design of heat to power systems. Two targeting procedures have been proposed.

A new algebraic targeting procedure has been proposed that allows to quickly determine the maximum theoretical amount of power that can be generated from sets of hot streams represented by hot composites in T-H space. The method takes the form of a simple problem table algorithm common in the field of process integration, which can be executed reliably and quickly. The thesis derived the underlying relationships of the procedure based on the assumptions necessary to determine the thermodynamic limits of infinite Carnot cycles. The proposed method was discuss with three illustrative example cases to explain its application and highlight its simplicity. The results highlight how targets vary significantly depending on the shape of the composites.

The proposed targeting method allows designers to quickly determine the theoretical limits for power generation from sets of multiple heat sources or hot composites. These limits cannot be outperformed by any power cycles in practice and can inform decision makers to justify (or not) additional time to pursue such power generation options in depth. Similar to other targeting methods in process integration, the proposed procedure would precede and motivate any detailed and time-consuming design studies.

A second targeting procedure has been developed to determine the maximum theoretical amount of power that can be developed from a set of hot streams. The second procedure was based on the use of the Rankine cycle. This method took into account the requirements of preheating and evaporation of the working fluid. Due to this consideration, the second method does give a lower target than the first targeting procedure. However, it provides a more realistic benchmark to design for.

In order to build on the current work, many assumptions that have been made in this work can be changed. For example, for the Carnot cycle targeting, the assumption that the lower temperature is constant was made. However, the assumption can be changed that the lower temperature is constant and not changing. This would change the power generation targeting. Another improvement that can be made for the Rankine cycle targeting is using multiple working fluids to determine what is the maximum power that can be generated when multiple working fluids are used.

The current work is limited by being unable to consider isothermal streams for the Rankine cycle targeting procedure. In addition, in order to get a true target for the Rankine cycle targeting procedure, an optimal fluid would need to be determined. This can be done by trying multiple working fluids and selecting the working fluids that give the highest efficiency.

REFERENCES

[1] Tchanche BF, Lambrinos G, Frangoudakis A, Papadakis G. Low-grade heat conversion into power using organic Rankine cycles - A review of various applications. Renew Sustain Energy Rev 2011;15:3963–79. doi:10.1016/j.rser.2011.07.024.

[2] Jiménez-Gutiérrez A, Lona-Ramírez J, Ponce-Ortega JM, El-Halwagi M. An MINLP model for the simultaneous integration of energy, mass and properties in water networks. Comput Chem Eng 2014;71:52–66. doi:10.1016/j.compchemeng.2014.07.008.

[3] Oluleye G, Jobson M, Smith R. A hierarchical approach for evaluating and selecting waste heat utilization opportunities. Energy 2015. doi:10.1016/j.energy.2015.05.086.

[4] Öhman H, Lundqvist P. Comparison and analysis of performance using Low Temperature Power Cycles. ApplThermEng2013;52:160–9. doi:10.1016/j.applthermaleng.2012.11.024.

[5] Minea V. Power generation with ORC machines using low-grade waste heat or renewable energy. ApplThermEng2014;69:143–54. doi:10.1016/j.applthermaleng.2014.04.054.

[6] Linnhoff B. Thermodynamic Analysis in the Design of Process Networks. ComputChemEng1979;3:283–91. doi:10.1016/0098-1354(79)80047-2.

[7] Dhole VR, Linnhoff B. Total site targets for fuel co-generation, emissions, and cooling. ComputChemEng1993;17:101–9. doi:10.1016/0098-1354(93)80214-8.

[8] Smith R. Chemical Process Design and Integration. 2$^{nd}$ ed. West Sussex: John Wiley and Sons Ltd; 2005.

[9] Boldyryev S, Varbanov PS. Low potential heat utilization of bromine plant via integration on process and Total Site levels. Energy 2015;90:47–55. doi:10.1016/j.energy.2015.05.071.

[10] Hackl R, Andersson E, Harvey S. Targeting for energy efficiency and improved energy collaboration between different companies using total site analysis (TSA). Energy 2011;36:4609–15. doi:10.1016/j.energy.2011.03.023.

[11] Klemeš J, Dhole VR, Raissi K, Perry SJ, Puigjaner L. Targeting and design methodology for reduction of fuel, power and CO2 on total sites. ApplThermEng1997;17:993–1003. doi:10.1016/S1359-4311(96)00087-7.

[12] Bungener S, Hackl R, Van Eetvelde G, Harvey S, Marechal F. Multi-period analysis of heat integration measures in industrial clusters. Energy 2015;93:220–34. doi:10.1016/j.energy.2015.09.023.

[13] Marechal F, Kalitventzeff B. Targeting the integration of multi-period utility systems for site scale process integration. ApplThermEng2003;23:1763–84. doi:10.1016/S1359-4311(03)00142-X.

[14] Stijepovic VZ, Linke P, Stijepovic MZ, Kijevčanin MLJ, Šerbanović S. Targeting and design of industrial zone waste heat reuse for combined heat and power generation. Energy 2012;47:302–13. doi:10.1016/j.energy.2012.09.018.

[15] Linnhoff B, Dhole VR. Shaftwork targets for low-temperature process design. ChemEngSci1992;47:2081–91. doi:10.1016/0009-2509(92)80324-6.

[16] Castier M. Rigorous multiple utility targeting in heat exchanger networks. Energy Convers Manag 2012;59:74–85. doi:10.1016/j.enconman.2012.02.019.

[17] Mavromatis SP, Kokossis AC. Conceptual optimisation of utility networks for operational variations - I. Targets and level optimisation. ChemEngSci1998;53:1585–608. doi:10.1016/S0009-2509(97)00431-4.

[18] Ghannadzadeh A, Perry S, Smith R. Cogeneration targeting for site utility systems. ApplThermEng2012;43:60–6. doi:10.1016/j.applthermaleng.2011.10.006.

[19] Goh WS, Wan YK, Tay CK, Ng RTL, Ng DKS. Automated targeting model for synthesis of heat exchanger network with utility systems. Appl Energy 2016;162:1272–81. doi:10.1016/j.apenergy.2015.04.113.

[20] Kapil A, Bulatov I, Smith R, Kim JK. Site-wide low-grade heat recovery with a new cogeneration targeting method. Chem Eng Res Des 2012;90:677–89. doi:10.1016/j.cherd.2011.09.001.

[21] Wan Alwi SR, Manan ZA. Simultaneous energy targeting, placement of utilities with flue gas, and design of heat recovery networks. Appl Energy 2016;161:605–10. doi:10.1016/j.apenergy.2015.06.013.

[22] Curzon FL. Efficiency of a Carnot engine at maximum power output. Am J Phys1975;43:22. doi:10.1119/1.10023.

[23] Ondrechen MJ, Andresen B, Mozurkewich M, Berry RS. Maximum work from a finite reservoir by sequential Carnot cycles. Am J Phys 1981; 49:681-5.

[24] Ibrahim OM, Klein SA, Mitchell JW. Optimum Heat Power Cycles for Specified Boundary Conditions. J Eng Gas Turbines Power 1991;113:514–21. doi:10.1115/1.2906271.

[25] Baik YJ, Kim M, Chang KC, Lee YS, Ra HS. Power maximization of a heat engine between the heat source and sink with finite heat capacity rates. Korean J Air Condition RefrigEng 2011; 23:556-61,

[26] Park H, Kim MS. Thermodynamic performance analysis of sequential Carnot cycles using heat sources with finite heat capacity. Energy 2014;68:592–8. doi:10.1016/j.energy.2014.02.073.

[27] Stijepovic MZ, Papadopoulos AI, Linke P, Grujic AS, Seferlis P. An exergy composite curves approach for the design of optimum multi-pressure organic Rankine cycle processes. Energy 2014;69:285–98. doi:10.1016/j.energy.2014.03.006.

[28] Anvari S, Jafarmadar S, Khalilarya S. Proposal of a combined heat and power plant hybridized with regeneration organic Rankine cycle: Energy-Exergy evaluation. Energy Convers Manag 2016;122:357–65. doi:10.1016/j.enconman.2016.06.002.

[29] Li T, Wang Q, Zhu J, Hu K, Fu W. Thermodynamic optimization of organic Rankine cycle using two-stage evaporation. Renew Energy 2015;75:654–64. doi:10.1016/j.renene.2014.10.058.

[30] Sadeghi M, Nemati A, Ghavimi A, Yari M. Thermodynamic analysis and multi-objective optimization of various ORC (organic Rankine cycle) configurations using zeotropic mixtures. Energy 2016;109:791–802. doi:10.1016/j.energy.2016.05.022.

[31] Yun E, Kim D, Lee M, Baek S, Yoon SY, Kim KC. Parallel-expander Organic Rankine cycle using dual expanders with different capacities. Energy 2016;113:204–14. doi:10.1016/j.energy.2016.07.045.

[32] Xu J, Liu C. Effect of the critical temperature of organic fluids on supercritical pressure Organic Rankine Cycles. Energy 2013;63:109–22. doi:10.1016/j.energy.2013.09.068.

[33] Papadopoulos AI, Stijepovic M, Linke P, Seferlis P, Voutetakis S. Multi-level Design and Selection of Optimum Working Fluids and ORC Systems for Power and Heat Cogeneration from Low Enthalpy Renewable Sources. Comput Aided Chem Eng 2012;30:66–70. doi:10.1016/B978-0-444-59519-5.50014-9.

[34] Chagnon-Lessard N, Mathieu-Potvin F, Gosselin L. Geothermal power plants with maximized specific power output: Optimal working fluid and operating conditions of subcritical and transcritical Organic Rankine Cycles. Geothermics 2016;64:111–24. doi:10.1016/j.geothermics.2016.04.002.

[35] Frutiger J, Andreasen J, Liu W, Spliethoff H, Haglind F, Abildskov J, et al. Working fluid selection for organic Rankine cycles – Impact of uncertainty of fluid properties. Energy 2016;109:987–97. doi:10.1016/j.energy.2016.05.010.

[36] Collings P, Yu Z, Wang E. A dynamic organic Rankine cycle using a zeotropic mixture as the working fluid with composition tuning to match changing ambient conditions. Appl Energy 2016;171:581–91. doi:10.1016/j.apenergy.2016.03.014.

[37] Brignoli R, Brown JS. Organic Rankine cycle model for well-described and not-so-well-described working fluids. Energy 2015;86:93–104. doi:10.1016/j.energy.2015.03.119.

[38] Thol M, Lemmon E.W., Span R. Equation of state for benzene for temperatures from the melting line up to 725 K with pressures up to 500 MPa. High Temperatures-High Pressures, 41:81–97, 2012.

[39] Sandler SI. Chemical, Biochemical, and Engineering Thermodynamics. $4^{th}$ ed. New York: John Wiley and Sons Ltd. 2006:A5.

APPENDIX A

This Appendix presents an alternative derivation of Equation (10) to determine the maximum theoretical work from a composite segment in a temperature interval [39]. This derivation is done with assumption that there is no pressure difference at the inlet and exit of the streams.

The steady state energy and entropy balances for interval j are given by

$$0 = H_i - H_{i+1} - W_j^{max} + Q_j \tag{A1}$$

$$0 = S_i - S_{i+1} + \frac{Q_j}{T_o} + S_j^{gen} \tag{A2}$$

Combining (A1) and (A2) yields

$$W_j^{max} + T_o S_j^{gen} = (H_i - H_{i+1}) - T_o(S_i - S_{i+1}) \tag{A3}$$

The entropy generated from the system ($S_j^{gen}$) will be zero as all stages in the Carnot cycle are reversible. Hence, the maximum amount of work that can be generated is

$$W_j^{max} = (H_i - H_{i+1}) - T_o(S_i - S_{i+1}) \tag{A4}$$

Equation(A5) is known as availability (Ψ), i.e.the maximum work output associated with any steady state process:

$$\Delta\Psi = \Delta H - T_o \Delta S \tag{A5}$$

Using partial derivatives, the relationship between the availability and temperature at constant pressure can be determined for interval j.

$$\left(\frac{\partial \Psi}{\partial T}\right)_P = \left(\frac{\partial \mathrm{H}}{\partial T}\right)_P - T_o\left(\frac{\partial \mathrm{S}}{\partial T}\right)_P \quad \text{(A6)}$$

$$\left(\frac{\partial \mathrm{H}}{\partial T}\right)_P = CP_j \quad \text{(A7)}$$

$$\left(\frac{\partial \mathrm{S}}{\partial T}\right)_P = \frac{CP_j}{T} \quad \text{(A8)}$$

Integration of Equation (A6) determines yields

$$\Delta\Psi_j = \int_{T_{i+1}}^{T_i} \left(CP_j\right) - T_o\left(\frac{CP_j}{T}\right)\, dT \quad \text{(A9)}$$

$$\Delta\Psi_j = CP_j(T_i - T_{i+1}) - CP_jT_L\left[\ln\left(\frac{T_i}{T_{i+1}}\right)\right] \quad \text{(A10)}$$

Equation (6) and Equation (A10) are equivalent, i.e. the difference in availability equates to the work obtained from an infinite number of Carnot cycles.

APPENDIX B

```
function [Minimize2] =
CompositeStreamRankineInfinite(mcp,Temperatures,Heat,TpTest,DT)
InitialTemperature=Temperatures(1);
Tstart=Temperatures(1)-DT;
Tp=Tstart-DT;
hMatrix=[];
mMatrix=[];
h00Matrix=[];
QMatrix=[];
Teff=557;
HeatAvailable=sum(Heat);
P=0;
Qt=0;
m=[];
TMatrix(1)=Tstart;
TMatrix(2)=Tstart;

%Mass Flow Rate General
for(i=1:((Tstart-TpTest)/DT)+1)

    mcpa=mcp(1);
    if(i>1)
        if(TMatrix(2*(i-1))<Temperatures(1) &&
TMatrix(i)>Temperatures(2))
            mcpa=mcp(1);
        end

        if(TMatrix(2*(i-1))<=Temperatures(2))
            mcpa=mcp(2);
            Temperatures(1)=[];
            mcp(1)=[];
        end
    end

    IntermediateHeat=0;

    if(i==1)
        [h00,hp,h0,h1,Efficiency]=IdealRankineCycle(Tstart,Tp,1);
        m(i)=mcpa*DT/(h1-h0);

        if(mcpa==0)
            m(i)=Q
        end
        Q=m(i)*(h1-h0);
        QMatrix(i)=HeatAvailable;
        QMatrix(i+1)=HeatAvailable-Q;
        h00Matrix(i)=h00;
        TMatrix(i)=Tstart;
        TMatrix(i+1)=Tstart;
    end
```

```
    if(i==2)
        h0prev=h0;
        [h00,hpprev,h0,h1,Efficiency]=IdealRankineCycle(Tstart,Tstart-
DT,1);

        [h00,hp,h0,h1,Efficiency]=IdealRankineCycle(Tstart-DT,Tstart-
2*DT,1);

        hMatrix(1,1)=hpprev;

        h00Matrix(i)=h00;

        m(i)=(mcpa*DT-m(i-1)*(h0prev-hpprev))/(h1-h0);
        QMatrix(i+1)=HeatAvailable-Q-m(i-1)*(h0prev-hpprev);
        TMatrix(i+1)=Tstart-DT;
        TMatrix(i+2)=Tstart-DT;
        Q=Q+m(i)*(h1-h0)+m(i-1)*(h0prev-hpprev);
        QMatrix(i+2)=HeatAvailable-Q;
    end

    if(i>=3)
        h0prev=h0;

        for(j=0:i-2)
        [h00,hpprev,h0,h1,Efficiency]=IdealRankineCycle(Tstart-
DT*j,Tstart-(i-1)*DT,1);
        hMatrix(i-1,j+1)=hpprev;
        end

        for(j=1:i-2)
           IntermediateHeat=IntermediateHeat+m(j)*(hMatrix(i-2,j)-
hMatrix(i-1,j));
        end
        [h00,hp,h0,h1,Efficiency]=IdealRankineCycle(Tstart-(i-
1)*DT,Tstart-i*DT,1);
        h00Matrix(i)=h00;

        m(i)=(mcpa*DT-m(i-1)*(h0prev-hMatrix(i-1,i-1))-
IntermediateHeat)/(h1-h0);
        QMatrix(2*i-1)=HeatAvailable-Q-m(i-1)*(h0prev-hMatrix(i-1,i-
1))-IntermediateHeat;
        Q=Q+m(i)*(h1-h0)+m(i-1)*(h0prev-hMatrix(i-1,i-
1))+IntermediateHeat;
        QMatrix(2*i)=HeatAvailable-Q;
        TMatrix(2*i-1)=Tstart-(i-1)*DT;
        TMatrix(2*i)=Tstart-(i-1)*DT;

    end
```

```
end
Qp=0;

Tstart=InitialTemperature-DT;

for(i=1:length(m)-1)

    [h0z,hp,h0,h1,Efficiency]=IdealRankineCycle(Tstart,TpTest-1,1);
    Qp=Qp+m(i)*(hp-h0z);
    Tstart=Tstart-DT;
end
[h0z,hp,h0,h1,Efficiency]=IdealRankineCycle(TpTest,TpTest-1,1);
Qp=Qp+m(length(m))*(h0-h0z);

Tstart=InitialTemperature-DT;

for(i=1:length(m)-1)

    [h0z,hp,h0,h1,Efficiency]=IdealRankineCycle(Tstart,TpTest-1,1);
    P=P+m(i)*(h1-h0z)*Efficiency/100;
    Qt=Qt+m(i)*(h1-h0z);
    Tstart=Tstart-DT;
end

    [h0z,hp,h0,h1,Efficiency]=IdealRankineCycle(TpTest,TpTest-1,1);
    Qt=Qt+m(length(m))*(h1-h0z);
    QMatrix=[QMatrix HeatAvailable-Qt];
    TMatrix=[TMatrix 298];
    Minimize2=0
         set(gca,'FontSize',30)
     plot(QMatrix,TMatrix,'LineWidth',5);
     xlabel('Heat (kW)')
     ylabel('Temperature (K)');
     hold on
     plot([0 3500 10100 11700], [350 400 460 500],'r','LineWidth',5);
     legend('Cold Composite Curve','Hot Composite
Curve','Location','east')
     P
```